

UC San Diego

UC San Diego Electronic Theses and Dissertations

Title

Identification of Glycogen Synthase Kinase-3 substrates in Dictyostelium discoideum

Permalink

<https://escholarship.org/uc/item/8qz828kp>

Author

Lin, Connie

Publication Date

2016

Peer reviewed|Thesis/dissertation

UNIVERSITY OF CALIFORNIA, SAN DIEGO

Identification of Glycogen Synthase Kinase-3 substrates in *Dictyostelium discoideum*

A Thesis submitted in partial satisfaction of the requirements for the degree Master of Science

in

Biology

by

Connie Lin

Committee in charge:

Professor Richard A. Firtel, Chair
Professor Amy Kiger
Professor Deborah Yelon

2016

Copyright

Connie Lin, 2016

All rights reserved.

The Thesis of Connie Lin is approved and it is acceptable in quality and form for publication and electronically:

Chair

University of California, San Diego

2016

TABLE OF CONTENTS

Signature Page	iii
Table of Contents	iv
List of Figures	v
List of Tables	vi
Acknowledgements	vii
Abstract of the Thesis.....	viii
I. Introduction	1
II. Results	10
III. Discussion	39
IV. Materials and Methods	44
References	48

LIST OF FIGURES

Figure 1: Life cycle of <i>Dictyostelium discoideum</i>	3
Figure 2: (Left) Dictyostelium streaming during development (Singh et al., 2014); (Right) Dictyostelium chemotaxis towards cAMP (S. Lee, R. Firtel, University of California, San Diego).....	4
Figure 3: Cloning strategy for GSK3 substrate candidate genes	14
Figure 4: Knockout construct design	15
Figure 5: PCR screening of genomic DNA for <i>gxcGG</i> null cells	16
Figure 6: <i>in vitro</i> kinase assay results of SogA	18
Figure 7: <i>in vitro</i> kinase assay results of GxcGG	19
Figure 8: Images of wild-type cells compared with knockouts	24
Figure 9: Developmental data for Ax2, including <i>gxcGG</i> overexpression	26
Figure 10: Developmental data for <i>sogA</i> ⁻ cells with <i>sogA</i> and its derivatives...	27
Figure 11: Developmental date for <i>gxcGG</i> null cell lines with over-expression of <i>gxcGG</i> and its mutant derivatives	29
Figure 12: Developmental data for Ax2, including <i>sogA</i> overexpression	31
Figure 13: GFP localization data for GxcGG overexpression in wild-type cells in random and chemotaxis <i>in vivo</i> assays	33
Figure 14: GFP localization data for GxcGG protein derivatives in <i>gxcGG</i> ⁻ in random and chemotaxis <i>in vivo</i> assays	34
Figure 15: GFP localization data for SogA overexpression in random and chemotaxis <i>in vivo</i> assays	35
Figure 16: Global Stimulation data for overexpression of GxcGG	36
Figure 17: Global Stimulation data for overexpression of SogA-2Ala and 2Glu derivatives	37
Figure 18: Global Stimulation of <i>gxcGG</i> strains in Ax2 and <i>gxcGG</i> ⁻ cells.....	38

LIST OF TABLES

Table 1: Phosphoproteomic data for selected GSK3 substrate candidates	11
Table 2: GSK3 substrate candidates	12
Table 3: Chemotaxis data for wild-type, knockouts, and overexpression of selected putative substrates	20

ACKNOWLEDGEMENTS

I would like to acknowledge the many people individuals who have assisted me in obtaining this Masters degree. First of all, I must thank my mentor, Professor Richard A. Firtel, for his support and giving me the privileged opportunity to be part of this lab.

Secondly, I would like to thank Dr. Jesus Lacal Romero for his daily guidance, patience and mentorship through this project. My contribution to this project would not exist if not for Dr. Lacal's supportive role in guiding me every step of the way.

Next, I would like to thank the members of Firtel lab for their support and counsel. I especially thank Susan Lee for her guidance and Kimberly Elizabeth Baumgardner for her hard help, tutorship, and invaluable assistance through my undergraduate and graduate years.

Lastly, I would like to thank my family and friends who have been my cheer team throughout my graduate career.

ABSTRACT OF THE THESIS

Identification of Glycogen Synthase Kinase-3 substrates in *Dictyostelium discoideum*

by

Connie Lin

Master of Science in Biology

University of California, San Diego, 2016

Professor Richard A. Firtel, Chair

Glycogen synthase kinase-3 (GSK3) is a highly conserved multifunctional kinase that regulates many cellular processes in eukaryotes, including cell motility, microtubule function, and cell differentiation (Frame et al., 2001). *Dictyostelium* GSK3, GskA, has been shown to be essential for chemotaxis (Teo R et al., 2010), although only one GskA substrate, Daydreamer, has been identified so far (Kölsch et al., 2013). Interestingly, the chemotaxis phenotype of Daydreamer null cells was not as severe as the one observed for *gskA*⁻ (GskA null) cells,

suggesting that there may be more proteins downstream GskA that are regulating chemotaxis. To identify direct downstream effectors of GSK3, a phosphoproteomic assay was performed before and after stimulation with the chemoattractant cAMP in wild-type and *gskA*⁻ cells (Kölsch et al., 2013). This investigation provided potential direct GSK3 substrate candidates, GxcGG and SogA, based on the phosphorylation of the GSK3 consensus sequence (s/tXXXs/t) in wild-type cells but not in *gskA*⁻ cells. Our results showed that GxcGG and SogA were phosphorylated in *in vitro* kinase assays by GSK3. Overall, both *sogA*⁻ and *gxcGG*⁻ cells displayed chemotaxis and developmental defects that resulted in incomplete fruiting body development. However they operate at different areas of the GSK3 signaling cascade as visualized by the cell membrane translocation of GFP tagged GxcGG and translocation to the cytosol of GFP tagged SogA during chemotaxis. My investigations suggest that SogA and GxcGG are substrates of GSK3 involved in the cAMP chemotaxis signaling pathway.

I. INTRODUCTION

Cell migration plays a significant role in the proper development and maintenance of multicellular organisms. This function is especially vital in biological processes such as immune system leukocyte migration and embryogenesis, where cellular motility is advantageous (Wang et al., 2011). Chemotaxis, or directed cell migration, occurs when a cell polarizes and migrates in response to a gradient of chemical signals in the environment. Chemical signals can be chemoattractants that attract cells towards the signal, or chemorepellents that repel the cells away from the signal (Vorotnikov, 2011). This chemical signal activates surface receptors which then initiate internal signaling pathways that result in polarized cell morphology (Meili and Firtel, 2003; Vorotnikov, 2011). Thus the transmission of external stimuli targets cytoskeleton remodeling to change cell shape through internal signaling pathways.

Chemotaxis is a complex process starting from the detection of the chemical signal to the signal transduction pathway within the cell and finally the processing of information to tell the cell which direction to move. Any malfunction in this machinery can cause chemotaxis defects such as diminished or augmented chemotactic movement. For instance, in the eukaryotic model organism *Dictyostelium discoideum*, *gskA* null cells have severe chemotaxis defects (Teo R et al., 2010; Kölsch et al., 2013), while in neutrophils, the knockdown or over-expression of Radil, a Rap1 effector involved in the β 2-integrin activation, increases chemotactic movement (Liu et al., 2012). Not only is the decrease in chemotaxis detrimental to key immune system responses, such as neutrophil migration, but so is the up-regulation of chemotaxis. Metastatic cancer cell movement shows detrimental and augmented chemotactic ability (Radulescu et al., 2012). Cancer cells can develop from stem cells that undergo irregular mitosis and uncontrollably amplify the number of malignant cells in the area. In the metastasis hypothesis, cancer cells acquire the ability to penetrate the primary tumor location and infiltrate the surrounding tissue and create another

tumor at the new site (van Zijl et al., 2011). The act of metastatic cells escaping through the basal membrane and into lymphatic or blood vessel is intravasation. The hypothesis of active intravasation states that metastatic cells follow nutrient gradients and migrate actively towards blood vessels (Ojalvo et al., 2010). This migration of metastatic cells is seen in breast carcinoma cell movement towards the secretion of epidermal growth factor from colony stimulating, tumor associated macrophages (TAMs) (van Zijl et al., 2011). In addition to metastatic cell migration, the chemotactic movement of progenitor cells has been studied in tissue regeneration following wounding. The augmented ability of progenitor cells to chemotax towards wound sites following porcine bladder extracellular matrix (PBEM) stimulation promotes tissue regeneration over the traditional scar formation (Mitchell et al., 2012). Therefore, if the process of chemotaxis is clearly understood, then this knowledge can be applied towards medical applications such as targeted intervention of cancer cell metastasis and wound closure.

Although many mammalian cell types utilize chemotaxis, the study of chemotaxis in human tissue culture is difficult (Cai et al., 2012). Instead, the slime mold *Dictyostelium discoideum* is a paradigm used for the study of chemotaxis due to similarities between this eukaryotic slime mold and many mammalian cell types, including leukocytes.

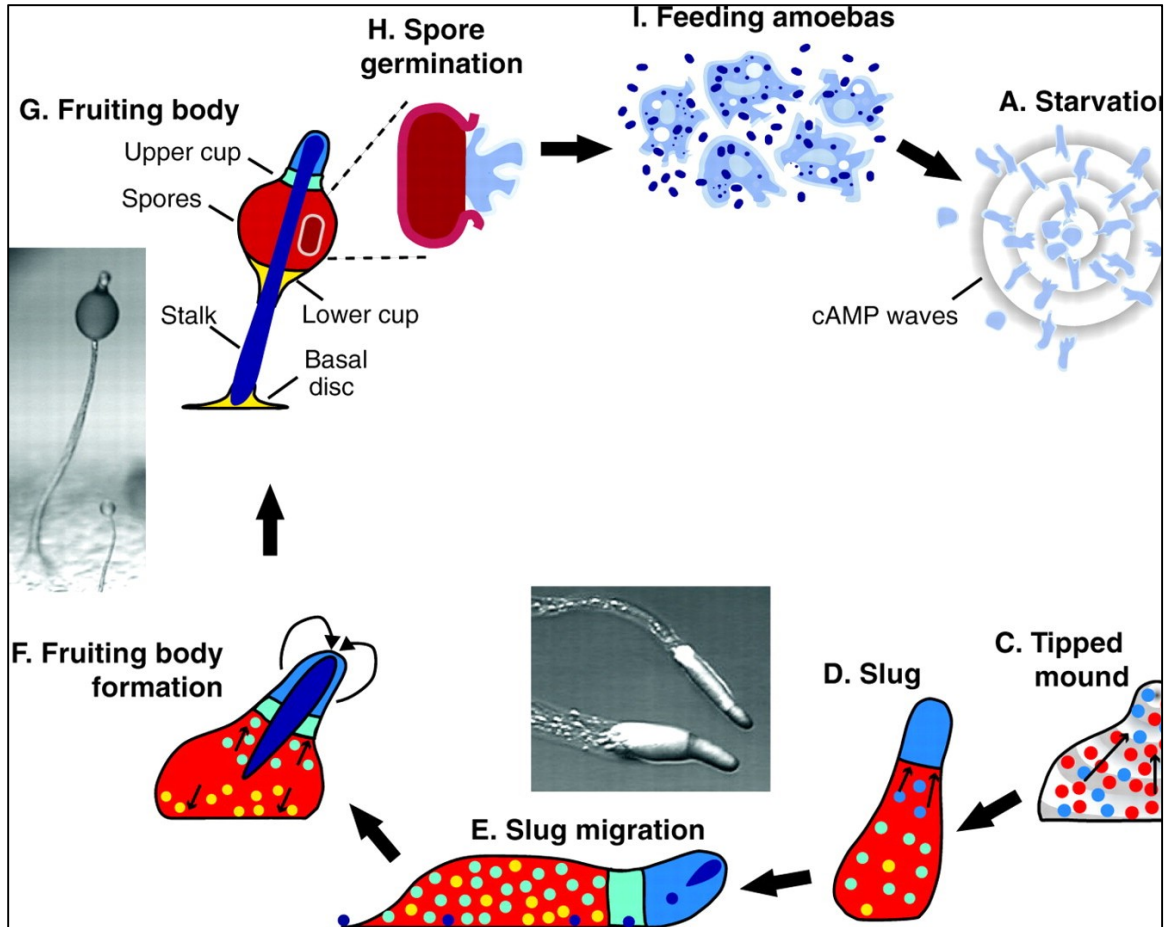


Figure 1: Life cycle of *Dictyostelium discoideum* (Schaap 2011). (A) Starving *Dictyostelium* secrete pulses of cAMP that causes (B) chemotactic aggregation of cells into the mound form. While in the mound, (C) cells continue to move upwards towards the continued cAMP emission resulting in a tipped mound. (D) This growth eventually becomes a slug which will fall over (E) and migrate. (F) Fruiting body formation starts when different cell types migrate to specific locations of the fruiting body. The fruiting body (G) ultimately differentiates into the support structures of the fruiting body the spores, and the stalk cells. (H) The spores germinate and resume proliferation as (I) individual cells.

Chemotaxis is observed during growth and development of *Dictyostelium* (Bonner et al, 1971). In the life cycle of *D. discoideum*, the slime molds alternate between periods of growth involving feeding and cell division as individual cells (vegetative state) and periods of development as cell aggregate when the bacterial food supply is depleted (Bonner, 1971). Vegetative *D. discoideum* cells feed on bacteria during growth and can move towards their

bacterial food sources by sensing the highest concentration of chemoattractant folic acid secreted from bacteria (Segota et al., 2013). When food is depleted, *D. discoideum* cells suffer from starvation and they will initiate a developmental program to survive (Figure 1). Under starvation, developed *D. discoideum* cells secrete their own chemoattractant cAMP to attract other starving cells (Schaap, 2011; Singh et al., 2014). Neighboring *Dictyostelium* will then respond to cAMP by migrating along the chemical gradient towards the highest concentration of cAMP signal and form aggregates and stream together (Schaap, 2011; Amselem et al., 2012; Lee and Firtel, Singh et al., 2014). This process in which *D. discoideum* cells sense and move towards cAMP is known as directed cell migration or chemotaxis. Eventually, the individual *Dictyostelium* cells act as a multicellular organism and transforming into stalks carrying spore cells forming a fruiting body (Schaap, 2011, Wang et al., 2011). The development of fruiting bodies is a survival mechanism to protect and disperse *Dictyostelium* spore cells to a new location when the environment is again suitable for growth.

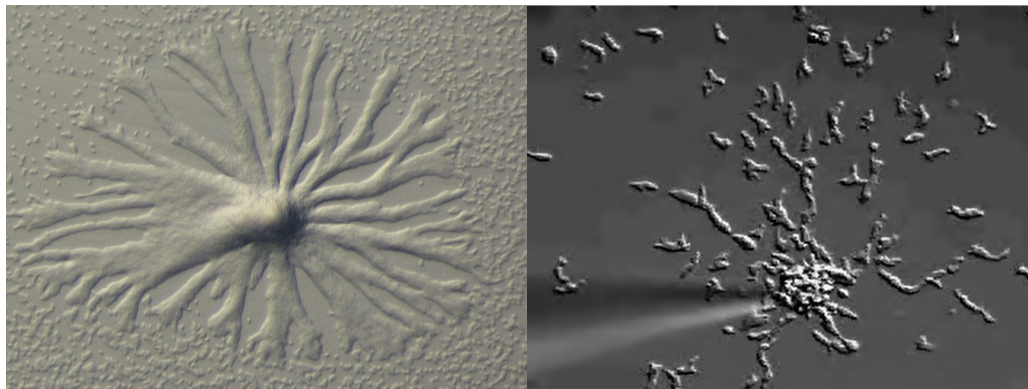


Figure 2: (Left) *Dictyostelium* cells streaming during development (Singh et al., 2014); (Right) Individual *Dictyostelium* cells chemotaxing towards cAMP (S. Lee, R. Firtel, University of California, San Diego)

Although mammalian systems do not commonly utilize cAMP or folic acid as chemoattractants, *D. discoideum* is a popular model system for the analysis of chemotaxis due to the similar internal signaling molecules and cytoskeletal regulators. *Dictyostelium* cells have

amoeboid movement, characterized by front-to-tail polarized morphology, moving towards a gradient of external stimuli, with the creation of a pseudopod on the side of the cell closer to the gradient (Haastert et al., 2009, Vorotnikov, 2011). Interestingly, amoeboid movement is the most common mode of locomotion in eukaryotic cells (Shi et al., 2013). For instance in humans, immune cells, such as white blood cells (leukocytes) including neutrophils, and metastatic cells are adept at amoeboid movement (Ojalvo et al., 2010). In fact, both free-living *D. discoideum* and leukocytes share common morphological structure of chemotactic signaling (Vorotnikov, 2011). In both cell types, polarization of the cell body is established following the detection of a signal gradient (Janetopoulos et al., 2008). In the cytoskeleton of leukocytes and *D. discoideum* cells, actin-rich structures form in the leading head of the cell, while myosin structures retract in the opposite direction (Lee et al., 2010). As *Dictyostelium* growth and development chemotaxis is easily induced, *Dictyostelium* is an excellent model for the research of the cytoskeleton and its regulation to allow proper cell migration.

Investigations into the mechanisms of chemotaxis have led to multiple different chemotaxis signaling pathways. These pathways affect protein recruitment to the leading edge and also to the back off the cells. The transmembrane cAMP G-protein coupled receptor (cAR) regulates the different pathways by sensing the cAMP in the extracellular environment and activating its associated G-protein when bound with the ligand (Xiao et al., 1997). During chemotaxis, phosphoinositol3-kinase (PI3K) is activated downstream of cAR. PI3K phosphorylates phosphatidylinositol (4,5)-biphosphate [PI(4,5)P₂] to create an intracellular gradient of phosphatidylinositol (3,4,5)-triphosphate [PI(3,4,5)P₃] (Sasaki and Firtel, 2006). This increased gradient of PI(3,4,5)P₃ at the leading edge of cells recruits other proteins to the leading edge. A separate chemotaxis related signal cascade has been studied to involve a protein complex called target of rapamycin complex 2 (TORC2) which phosphorylates downstream proteins PKB and PKBR1 phosphorylates downstream proteins PKB and PKBR1 (Lee et al., 2005; Charest et

al., 2010). The TORC2 and PI(3,4,5)P₃ pathways activate and recruit proteins to the leading edge, however there are also pathways involved in chemotaxis that regulate myosin to retract to the back of the cell wall (Mondal et al., 2008). Our investigation hopes to find how Glycogen synthase kinase-3 is involved with other chemotaxis signaling cascades and how it is involved in chemotaxis.

Glycogen synthase kinase-3 (GSK3) is a highly conserved protein kinase in eukaryotes involved in many cell processes including metabolism, cell differentiation, motility and development (Kim et al., 2011). In mammalian cells, GSK3 is needed for the regulation of many signaling pathways such as Wnt and inositol-PIP₂ (Radulescu et al., 2012, Frame et al., 2001). The GSK3 homologue in *Dictyostelium* is GskA, encoded by *gskA*. Recent data show that the loss of GskA in *D. discoideum* diminishes the cells ability to chemotax towards the chemoattractants cAMP and folate (Teo et al., 2010). Phenotypic changes in *gskA* null cells include slower movement and decreased directionality when compared with its wild-type counterparts (Kim et al., 2011; Kölsch et al., 2013). Studies have shown a reduced assembled myosin II (MyoII) response in *gskA* null cells, in addition to lower phosphatidylinositol (3,4,5)-triphosphate production (Teo et al., 2010). The *gskA* null cells have higher recruitment of PI3K to the plasma membrane and increased activation of the PKB and kinase PKBRI signaling pathways (Teo et al., 2010). Furthermore, in the cAMP-dependent activation pathway of GskA, ZAK2 has been identified as a tyrosine kinase that regulates GskA for cell differentiation, migration and polarity (Kim et al., 2011). Despite the fact that the number of GskA substrates is assumed to be large, only a few direct downstream effectors of GskA regulating chemotaxis are known.

Here is what is known about GSK3 and its substrates. GSK3 commonly phosphorylates serine and threonine residues within a substrate protein with the S/TPXXS/TP consensus sequence, where the X is any amino acid, S is serine, T is threonine, and P is proline (Fiol et al., 1988). Many potential GSK3 substrates require priming, or the pre-phosphorylation, optimally 4

amino acids C-terminal from the GSK3's target amino acid (Sutherland, 2011). Thus, this sequence can be used to identify potential GSK3 substrates. Currently there are two GSK3 substrates involved in chemotaxis identified in *Dictyostelium discoideum*: Daydreamer and PI3K (Kölsch et al., 2013, Sun et al., 2013). Daydreamer (DydA) is a Ras effector involved in chemotaxis cell polarization and directional movement (Kölsch et al., 2013). Studies suggest DydA as a negative regulator of PKB and PKBR1 activation loop, and F-actin production and assembled myosin II due to increased activation of the signaling pathways in Daydreamer null cells (Kölsch et al., 2013). Interestingly, cells lacking Daydreamer have shown chemotactic defects, but not as severe as *gskA* null cells (Kölsch et al., 2013). Since the Daydreamer null cells display less chemotactic ability compared to *gskA* null cells, we hypothesized that other additional substrates downstream of GSK3 may exist that contribute to cell motility. The other identified substrate of GSK3 is phosphatidylinositol-3-kinase 1 (PI3K). Studies show that GSK3 is essential for proper membrane localization of PI3K (Sun et al., 2013). In *gskA* null cells, PI3K has decreased protein localization to the membrane and inefficient polarization of the cell during chemotaxis (Sun et al., 2013). Phosphomimetic substitutions of GSK3 consensus sites on PI3K restores cAMP induced membrane transient translocation in *gskA* null cells compared with wild-type (Sun et al., 2013). This study shows that GSK3 dependent phosphorylation is important for cAMP depend localization of PI3K to the membrane.

In the context of these findings, the question I am studying comes into sight. My goal is to identify new substrates of GskA in response to the chemoattractant cAMP, involved in chemotaxis, in the model organism *D. discoideum*. I started this project by using bioinformatics to analyze the phosphoproteome of wild-type and *gskA* null cells to identify potential substrates of GskA (Kölsch et al., 2013). Proteins containing phosphopeptides with the S/TPXXS/TP consensus site that were phosphorylated in wild-type cells but not in *gskA* null cells were selected for further analysis. One of the candidate proteins, GxcGG, encoded by the *gxcGG* gene is

suggested to be involved in the regulation of cytoskeleton remodeling due to the pleckstrin homology domain, which is a protein domain that occurs in an array of intracellular signaling proteins or in cytoskeletal proteins (Zhang et al., 2010). The protein GxcGG is also a guanine exchange factor (GEF) for rac protein. Guanine exchange factors are proteins that activate GTPases by stimulating the release of guanine diphosphate (GDP) so that guanine triphosphate (GTP) can bind. GTPase-Activating Proteins (GAPs) are another family of regulatory proteins that function to stimulate GTPases to hydrolyze GTP into GDP. GO annotations suggest that the other candidate protein, SogA, encoded by the *sogA* gene is involved in the regulation of cytoskeleton remodeling due to its kelch repeats. Although little is currently known about kelch repeats, the domain is presumably involved in protein-protein interaction via multiple kelch repeats that create a β -propeller structure (Philips, 1998). Both GxcGG and SogA, were ultimately selected for further analysis due to their decrease in phosphorylation in *gskA* null cells compared with wild-type, seen in the proteomics assay data, and predicted domains correlating to known cytoskeleton proteins from bioinformatics.

In order to study the relationship of these candidate proteins to GSK3, I performed a kinase assay in the presence of the immunoprecipitated proteins (GxcGG and SogA) and human recombinant GSK3 to determine if these candidates are phosphorylated *in vitro* by GSK3. In addition, this *in vitro* kinase assay was also done with the immunoprecipitated proteins containing mutations to alanine, in the primed and GSK3 sites, to examine whether or not these sites are the specific phosphorylation sites for GSK3. The alanine substitution in a potential phosphorylation site in any given protein is supposed to prevent protein phosphorylation from its cognate kinase. Similarly, the GSK3 and priming sites were mutated to aspartate to imitate phosphorylation in a manner similar to how Leger tested the protein tau for phosphorylation (Leger et al., 1997). Whereas the alanine mutant derivatives were tested both *in vitro* and *in vivo*, the aspartate mutants were tested only *in vivo*. Once these substrates were validated with the kinase assays,

my next question was to understand their effect on chemotaxis and development in *D. discoideum*. Using homologous recombination, the *gxcGG* and *sogA* genes were knocked out to examine their effects on cell motility *in vivo* studies using time-lapse microscopy techniques, and analyzed with Dynamic Image Analysis System (DIAS) to see motile behavior changes with respect to wild-type cells. I expressed the wild-type and mutant (alanine or aspartate) constructs in the *D. discoideum* wild-type and null strains to see if the mutant and wild-type proteins can complement the null phenotypes and to examine the effects of protein over-expression. In addition, both the mutants and wild-type proteins were tagged with GFP to examine their subcellular localization.

I believe this study further elucidates the knowledge of *D. discoideum* cAMP chemotaxis pathway and assist in providing a better understanding of cell motility utilized by an array of mammalian cell types including leukocytes and metastatic cancer cells.

II. RESULTS

Phosphoproteomics identify potential GskA substrates involved in chemotaxis in *Dictyostelium discoideum*

Phosphoproteomic mass spectrometry analysis was performed on wild-type (Ax2 strain) and *gskA*⁻ (GskA null) cells to compare levels of protein phosphorylation changes between the two strains that may be dependent on stimulation with the chemoattractant cAMP (Kölsch et al., 2013). Briefly, the proteome of each strain was obtained at three different time points, before (0 sec) and after (10 and 60 sec) cAMP stimulation. Then, potential direct GskA substrates were selected from the analysis based on phosphorylation levels (spectral numbers obtained from proteomics) in the potential GSK3 consensus site S/TPXXS/TP containing peptides. These selected GSK3 substrates are phosphorylated in wild-type cells, but not phosphorylated (or severely reduced) in the *gskA*⁻ cells. We also based our criteria on whether the proteins do not contain transmembrane domains, and the presence of domains that are related to cAMP signaling and regulation of chemotaxis. From the most promising candidates that showed decreased phosphorylation in *gskA*⁻ cells, SogA (DDB0191741) and GxcGG (DDB0233491) proteins were selected for further analysis. The phosphoproteomic data in Table 1 show that peptides containing the GSK3 consensus site presented phosphorylation over time in wild-type cells. Spectra changes of SogA started from no detection at 0 seconds, to spectra of 8 and 4, at 10 and 60 seconds, respectively. On the other hand, the spectra remained undetectable for the same SogA peptide chain in *gskA*⁻ cells (Table 1). In wild-type cells, the GxcGG peptide had spectra of 3 at 0 seconds and no detection at 10 and 60 seconds, whereas the same phosphosites were not detected in *gskA*⁻ cells (Table 1). According to our phosphoproteomics data, the potential phosphosites for GSK3 phosphorylation and the corresponding priming phosphorylation are T753 and S757 in GxcGG, and S565 and S569 in SogA.



Table 1: Phosphoproteomic data for the selected GSK3 substrate candidates. The number of spectra indicates degree of phosphorylation detected from the peptide sequences. “nd” indicates no detection. Lower-case letters within peptide sequence indicates specific phosphorylation site detected by mass spectrometry. The consensus GSK3 site is underlined.

SogA	Ax2			<i>gskA</i>			Peptide
Time (seconds)	0s	10s	60s	0s	10s	60s	
Spectra	nd	8	4	nd	nd	nd	DLAFSMNGNNLs <u>PQG</u> sPHLNSNQR
Spectra	3	3	3	3	3	1	RVNsTDSVIIDGR
Spectra	3	3	3	nd	1	3	VNsTDSVIIDGR
GxcGG	Ax2			<i>gskA</i>			Peptide
Time (seconds)	0s	10s	60s	0s	10s	60s	
Spectra	3	nd	nd	nd	nd	nd	DKWVSVLNDLQQQLt <u>PPP</u> sPTLSR
Spectra	nd	1	2	nd	nd	nd	FTGSLsPTLK
Spectra	nd	3	nd	nd	nd	nd	WVSVLNDLQQQLtPPPSPTLSR

In silico characterization of the selected candidates

The amino acid sequences of GxcGG and SogA were inputted into Prosite-ExPasy in order to generate diagrams of their domains (Table 2). GxcGG is a 89kDa protein containing the PH domain and DH_2 domain. SogA is a 80kDa protein with four kelch repeats clustered closer to the N-terminus.

Table 2: Selected GskA substrate candidates. Sequence characterization diagram shows the domains of the candidate proteins. Protein GxcGG is known to contain a RhoGEF and Pleckstrin Homology domain. Protein SogA is known to contain Kelch repeats.

Candidate Protein	Sequence Characterization	Known Functions
GxcGG (89 kDa)		PH domain and a DH_2 domain containing protein
SogA (80 kDa)		Unknown. Protein with Kelch repeats

DNA amplification and cloning – creating pBluescript:gene constructs for knockout generation and site directed mutagenesis.

The goal of creating knockout strains in the genes *gxcGG* and *sogA* was to conduct *in vivo* experiments to see whether or not development and chemotaxis was affected in the null cells, compared to wild-type cells. GSK3 substrate genes were cloned in pBluescript (pBS) SK vector in order to create knockout strains via homologous recombination, and I also used these SK-*gxcGG* and SK-*sogA* construct to carry out PCR site-directed mutagenesis to mutate the GSK3 consensus sites. For the generation of the knockouts, the *gxcgg* and *soga* genes were functionally disrupted with the insertion of a BlasticidinS-resistance (BSR) cassette, and the resulting constructs were electroporated back into wild-type cells (Figure 3). All candidate genes were cloned from genomic DNA through the use of PCR (Figure 4). After electroporation, cells were selected with HL5 media containing blasticidin. Then, to isolate individual cell colonies, cells were diluted and grown on a bacteria plate to a final cell density of 50 to 100 cells per plate. Single *Dictyostelium* colonies were then transfer to 24 well plates with HL5 media and

supplemented with blastidicin (to minimize the presence of wild-type cells) and with ampicillin (to kill any possible bacteria residue). After two days growing colonies were transfer to petri plates and after two more days genomic DNA was extracted. To genetically screen each genomic DNA, a template for PCR with primers hybridizing to inside and outside of the BSR cassette was used (Figure 4). PCR DNA was subsequently run on agarose gels to determine the correct insertion of the BSR cassette into the genome (Figure 5). Expected *gxcGG* and *sogA* DNA length of PCR fragments are 2,151 base pairs for gene *sogA* and 2,391 base pairs for gene *gxcGG*. These PCR lengths are indicated in Figure 4

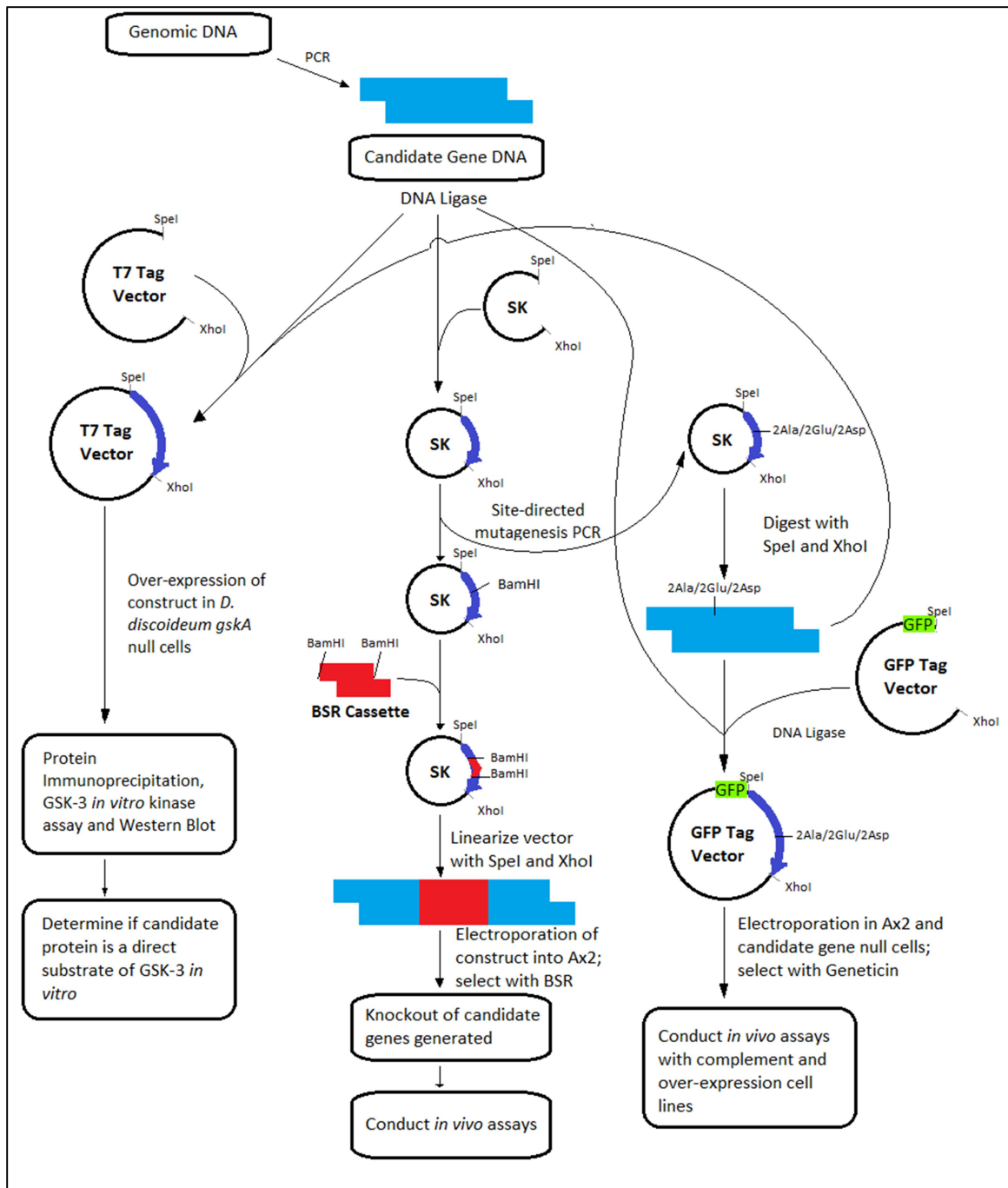


Figure 3: Cloning strategy for GSK3 substrate candidate genes. Shown above are steps for cloning to generate knockouts, create proteins for GSK3 phosphorylation, and create site-directed mutated proteins for chemotaxis and GFP localization. 2Ala/2Glu/2Asp indicates the double point mutations of the consensus site.

Figure 5 shows the PCR results of successfully constructed *gxcGG* by insertion of the BSR cassette. The knock-out constructs of *gxcGG* would contain the BSR cassette within the gene and increase the PCR product to the length of 3,891 base pairs. In Figure 5, the columns 4, 5, 6, 7 and 8 are separate PCR products showing lengths of 3,891, but not the band corresponding to wild-type *gxcGG*, indicative of successful gene knockouts of *gxcGG*.

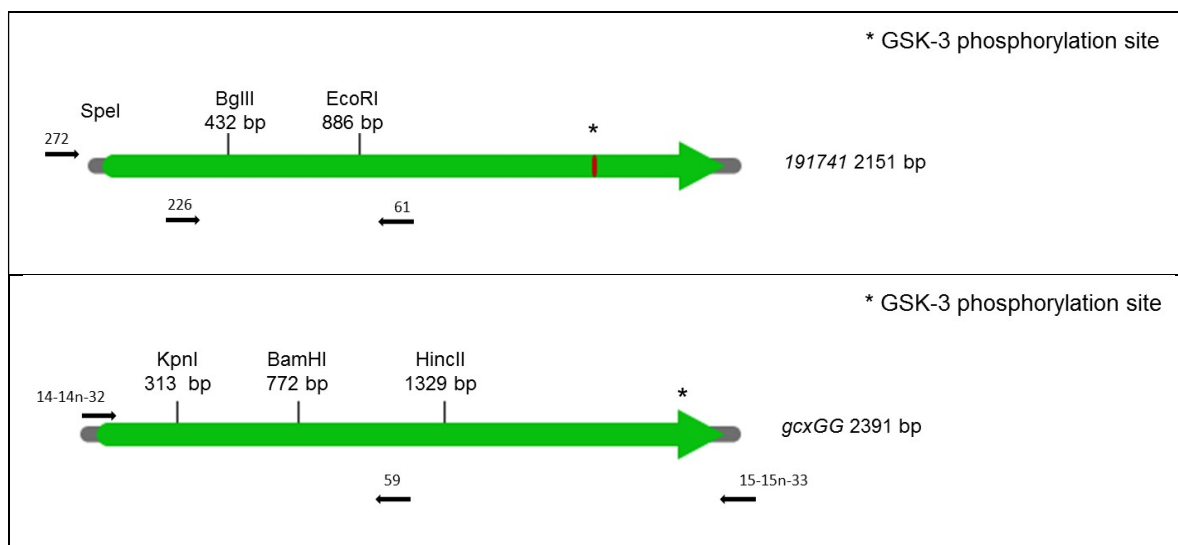


Figure 4: Knockout construct design. Arrows with numbers above correlate to the primers used for PCR to screen for knockout success. The BamHI restriction site is where the BSR cassette was inserted to create the gene knockout.

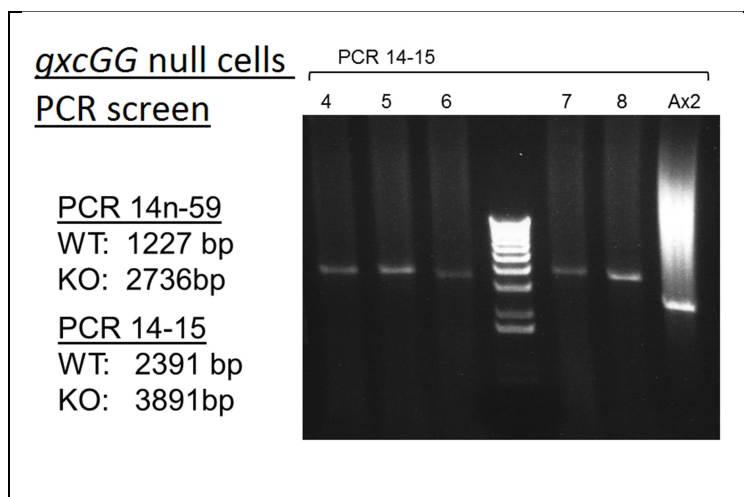


Figure 5: PCR screening of genomic DNA for *gxcGG* null cells. Agarose gel containing PCR products made from different primers and different strains of genomic DNA. Different primers were created to match each gene. Using these primers, the presence of the BSR cassette within a gene versus wild-type gene was confirmed with PCR.

Site-directed mutagenesis was used to introduce alanine (A) point mutations for *in-vitro* phosphorylation assays and alanine (A) and aspartate (D) (or glutamate [E]) point mutations for localization assays into the GxcGG and SogA proteins. The T753A and S757A mutations on GxcGG, and S565A and S569A mutations on SogA silenced the consensus site from GSK3 modification. The T753E and S757E mutations on GxcGG and S565D and S569D mutations on SogA mimicked the phosphorylation by GskA. Genes with the demarcation “2 Ala” meant that the GSK3 consensus site was silenced and unable to be phosphorylated. Genes with the demarcation “2Asp” or “2 Glu” meant that the consensus site mimicked phosphorylation. Next, wild-type GxcGG and SogA, and their point-mutated derivative genes were ligated with a vector that added to the proteins a GFP tag N-terminal. Similar strategy was carried out to tag GxcGG, SogA and their A mutant to a T7 tag N-terminal. The resulting products successfully created were GFP-*gxcGG*, GFP-*gxcGG*-2Ala, GFP-*gxcGG*-2Glu, GFP-*sogA*, GFP-*sogA*-2Ala, GFP-*sogA*-2Asp, T7-*sogA*, T7-*gxcGG*, T7-*sogA*-2Ala and T7-*gxcGG*-2Ala. The resulting recombinant plasmids were electroporated into wild-type cells and their respective null cells. The T7 tagged

proteins were generated for the kinase *in vitro* assay, whereas the GFP tagged proteins were used in *in vivo* assays of chemotaxis and to monitor the GFP localization of the proteins.

GxcGG and SogA are phosphorylated by human recombinant GSK3 at Thr753 and Ser757 on GxcGG and Ser565 and Ser569

The *gxcGG* and *sogA* PCR gene products were also subsequently digested and ligated into an N-terminal T7 tag vector, as outlined in Figure 3, to generate T7-tagged proteins. The resulting constructs were then electroporated into *gskA*⁻ cells for overexpression of the GxcGG and SogA recombinant protein. In order to determine if T7 tagged GxcGG and SogA are directly phosphorylated by GSK3, T7-GxcGG and T7-SogA were overexpressed in *gskA*⁻ cells and then immunoprecipitated using T7-agarose beads that pulled down the T7-tagged GxcGG and SogA proteins. Then, the immunoprecipitated T7-GxcGG and T7-SogA were incubated in the absence and the presence of human recombinant GSK3 and gamma 32P (as described in M&M). Figure 6 shows that protein SogA is phosphorylated in the presence of GSK3, but its phosphorylation is much reduced in the absence of GSK3. Furthermore, protein levels of the SogA sample were normalized between the samples incubated with and without GSK3. Our results suggest that the relative phosphorylation of SogA in the presence of GSK3 is higher than in its absence. These results suggest that SogA is a direct substrate of GSK3 *in vitro*.

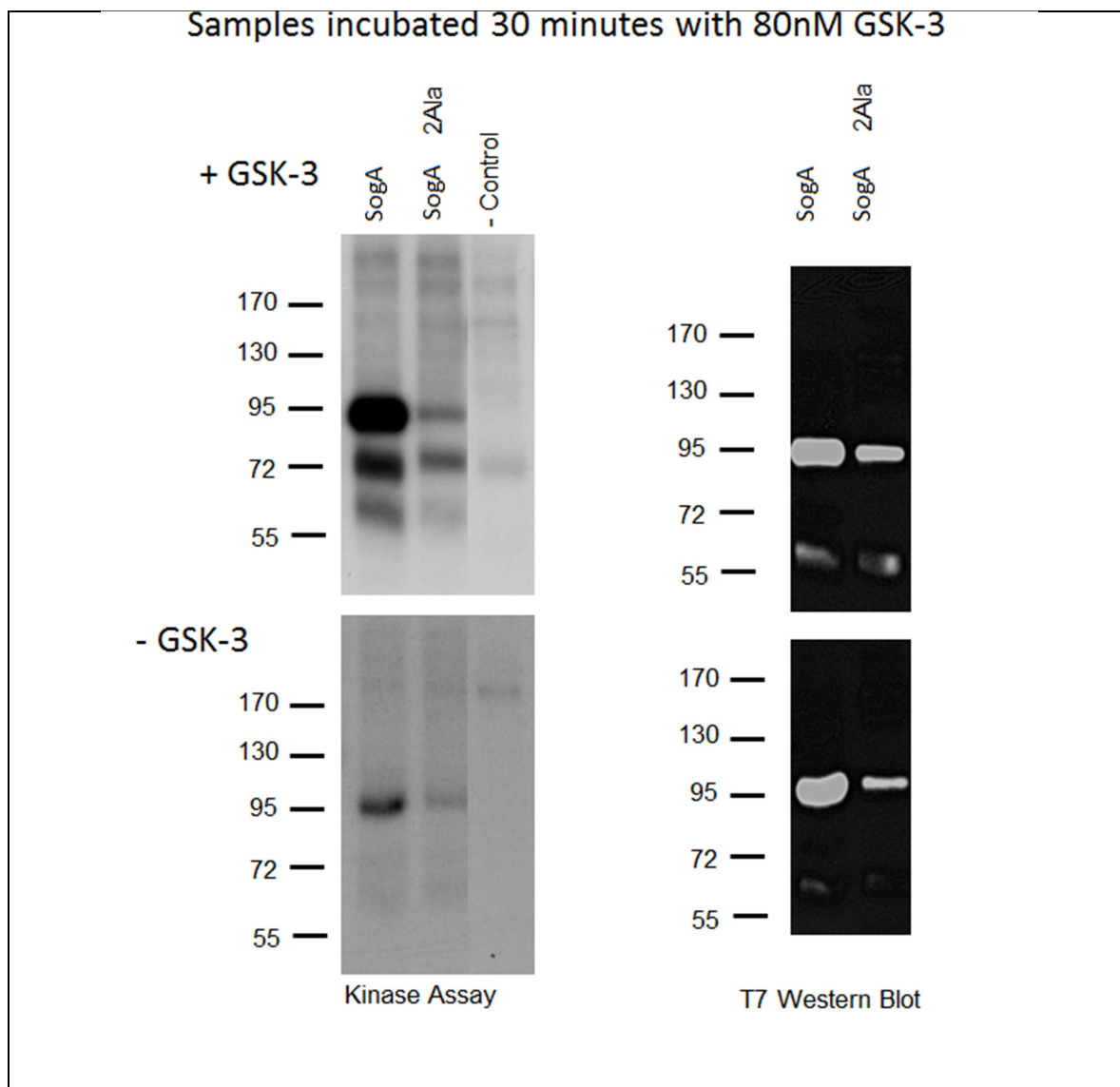


Figure 6: *in vitro* kinase assay results for SogA. Note relative decreased phosphorylation of SogA 2Ala (SogA with Alanine mutated consensus site) in comparison with SogA in the presence of GSK3. There is a significant decrease of phosphorylation of both SogA and SogA 2Ala in samples lacking GSK3. T7 Western Blot indicates total protein level in the Western Blot.

To corroborate the phosphorylation sites of GSK3 in SogA, the *in vitro* kinase assays were performed with wild-type SogA proteins along with its alanine mutant derivatives at both the primed and GSK3 phosphorylation sites. Comparison of the wild-type and mutant SogA proteins shows that mutant SogA-2Ala has less relative phosphorylation levels compared to the wild-type SogA, suggesting that Ser565 and Ser574 constitute the GSK3 and priming site, respectively.

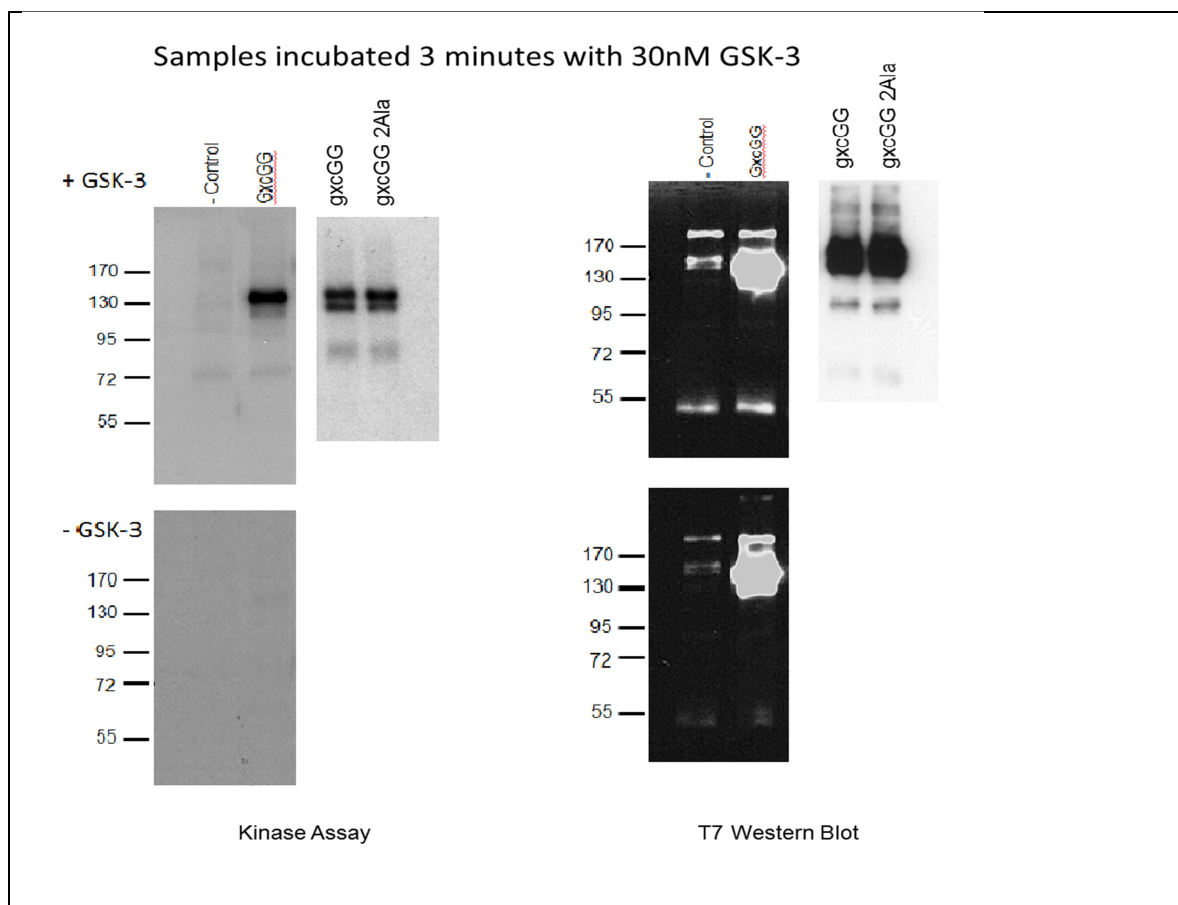


Figure 7: *in vitro* kinase assay results for GxcGG. Samples of GxcGG and GxcGG 2Ala incubated with and without GSK3 show that phosphorylation of GxcGG and its derivative proteins is increased in presence of GSK3 and not phosphorylated in the absence of GSK3.

Similar to SogA, phosphorylation levels of GxcGG were much higher in the presence of GSK3 than in its absence (Figure 7), suggesting that GSK3 is phosphorylating GxcGG *in vitro*. However, the samples containing GxcGG and GxcGG-2Ala are equally phosphorylated in the presence of GSK3, suggesting that the predicted GSK3 consensus sequence in GxcGG might not be unique for GSK3 or perhaps that due to the high number of potential GSK3 sites in GxcGG, other sites may be phosphorylated by the kinase *in vitro*.

Table 3: Chemotaxis data for wild-type, knockouts, and overexpression of selected putative substrates. Parameters determined by tracing individual cells using DIAS software. Values bolded indicate reduced speed of knockout strains compared with wild-type speeds.

Strain	N ^o of cells analyzed	Directionality	Speed ($\mu\text{m}/\text{min}$)	Direction change (deg)	Roundness (%)
Ax2 (Wild-type)	10	0.71 \pm 0.05	13.4 \pm 1.25	30.61 \pm 3.40	39.05 \pm 3.82
<i>gxcGG-</i>	15	0.55 \pm 0.12	8.03\pm1.39	46.45 \pm 9.47	36.83 \pm 3.97
<i>gxcGG- GFP-gxcGG</i>	12	0.41 \pm 0.08	5.18 \pm 0.79	58.48 \pm 5.13	31.26 \pm 5.35
<i>gxcGG-GFP-gxcGG-2Ala</i>	14	0.45 \pm 0.10	7.09 \pm 1.95	52.03 \pm 7.32	39.75 \pm 7.94
<i>gxcGG-GFP-gxcGG-2Glu</i>	11	0.55 \pm 0.08	7.32 \pm 1.38	48.38 \pm 8.60	33.85 \pm 4.83
Ax2 GFP- <i>gxcGG</i>	10	0.54 \pm 0.13	9.97 \pm 2.43	40.15 \pm 7.31	40.84 \pm 4.68
Ax2 GFP- <i>gxcGG-2Ala</i>	15	0.49 \pm 0.08	6.19 \pm 0.87	51.56 \pm 7.01	34.35 \pm 2.94
Ax2 GFP- <i>gxcGG-2Glu</i>	13	0.29 \pm 0.16	3.68 \pm 0.70	65.49 \pm 10.76	51.96 \pm 8.12
<i>sogA-</i>	15	0.66 \pm 0.09	8.89\pm1.83	36.70 \pm 8.30	31.42 \pm 4.61
<i>sogA- GFP-sogA</i>	10	0.52 \pm 0.12	5.51 \pm 0.90	49.55 \pm 9.28	46.56 \pm 6.72
<i>sogA- GFP-sogA -2Ala</i>	10	0.62 \pm 0.11	7.85 \pm 2.15	37.32 \pm 8.88	44.06 \pm 4.79
Ax2 GFP- <i>sogA</i>	15	0.60 \pm 0.06	6.17 \pm 1.12	43.81 \pm 7.88	45.30 \pm 9.02
Ax2 GFP- <i>sogA-2Ala</i>	10	0.56 \pm 0.14	7.51 \pm 1.38	44.18 \pm 10.82	37.59 \pm 3.03
Ax2 GFP- <i>sogA-2Asp</i>	11	0.48 \pm 0.10	6.70 \pm 1.36	43.57 \pm 8.94	42.35 \pm 6.09

Chemotaxis and Development of *gxcGG* and *sogA* null cells

Chemotaxis and development assays of *sogA* and *gxcGG* null cells were performed and compared to wild-type cells to determine if SogA and GxcGG participate in cell migration. Due to the severe chemotaxis defects of *gskA-* cells we expect potential GSK3 substrates to have less severe phenotypes, as observed for Daydreamer (Kölsch et al., 2013). Table 3 shows the results of the chemotaxis assays comparing the directionality, speed, direction change, and roundness of wild-type, *sogA*, and *gxcGG* null cells. The chemotaxis assays were performed as detailed in

Materials and Methods. Data was collected by tracing individual cells from chemotaxis movies using DIAS software. The *gxcGG*⁻ and *sogA*⁻ cells showed approximately a 35-40% decrease in speed compared to wild-type cells (Table 3). Also, both null cell types show a 0.8 to 0.9 fold decrease in directionality and a 0.8 to 0.9 fold decrease in roundness compared to wild-type cells. The *gxcGG* and *sogA* null cells showed an increase in the degree of direction change (1.5 and 1.2 fold, respectively), most notably in *gxcGG* null cells. In addition, there is a notable decrease in percent roundness in *sogA* null cells in comparison with wild-type cells. These effects suggest that SogA and GxcGG may have roles in the signal transduction pathways of chemotaxis toward cAMP.

Seeing how the *gxcGG* and *sogA* null cells presented chemotaxis defects such as decreased speed, we next tested for the complementation and over-expression of GxcGG and SogA in wild-type cells. In order to determine whether phosphorylation of GxcGG and SogA by GSK3 had an effect in how the proteins regulate chemotaxis and development, we also overexpressed GxcGG and SogA derivative mutants in their respective null strains.

We hypothesized that over-expression of *gxcGG* would restore the null phenotype of *gxcGG*⁻. However, this was not the case; over-expression of *gxcGG* in *gxcGG* null cells had a negative impact in directionality, speed, direction change and roundness (Table 3). For instance, the speed of *gxcGG*⁻ over-expressing GxcGG showed a 0.6 decrease compared to wild-type (Table 3). I hypothesized that over-expression would have a result between wild-type and the *gxcGG*⁻ cell line, however the opposite was revealed. The strain, *gxcGG*⁻GFP *gxcGG*, had a speed that was a 0.387 fold decrease from wild-type (Table 3). This speed was slower than that of the *gxcGG*⁻ cell line compared with wild-type. Over-expression of *gxcGG* with GFP-*gxcGG* 2Ala and GFP-*gxcGG* 2Glu plasmids yielded cells that were similar to *gxcGG*⁻ cell's chemotactic changes with a 0.529 to 0.546 fold decrease in speed, a 0.634 to 0.775 fold decrease in directionality, and a 1.58 to 1.70 fold increase in direction change in comparison with wild-type (Table 3). There

was no difference in roundness between wild-type and in the strain *gxcGG*GFP *gxcGG* 2Ala, however there was a 0.868 fold decrease in roundness in the overexpression strain, Ax2 GFP-*gxcGG* 2Glu (Table 3).

Overexpression of GFP-*gxcGG* in wild-type cells had a negative impact in chemotaxis with a 0.7 fold decrease in speed, 0.7 fold decrease in directionality, and a 1.3 fold increase in direction change (Table 3). Overexpression of the mutant derivatives GFP-*gxcGG* 2Ala and GFP-*gxcGG* 2Glu in wild-type also had a negative effect in the chemotaxis phenotype compared to wild-type, *gxcGG* null cells, and Ax2 GFP-*gxcGG* in regards to decreased speed, decreased directionality, and increased roundness (Table 3). Ax2 GFP-*gxcGG* 2Glu had the most dramatic change in directionality (0.4 fold decrease), speed (0.3 fold decrease), direction change (2.1 fold increase) and roundness (1.3 fold increase) compared to wild-type (Table 3). Our results suggest that overexpression of GxcGG and its derivatives have a negative impact in chemotaxis.

Over-expression of *sogA* with GFP-*sogA* and GFP-*sogA* 2Ala plasmids into *sogA*⁻ cells also suggested that SogA has a negative impact on chemotaxis with a 0.4 to 0.6 fold decrease in speed, a 0.7 to 0.9 fold decrease in directionality, and a 1.2 to 1.6 increase in direction change and a 1.1 to 1.2 increase in roundness (Table 3). The *sogA*⁻ GFP-SogA2Asp cells were not successfully generated because the cells would die shortly after electroporation GFP-*sogA*-2Asp containing plasmid.

Similar results were obtained for the overexpression of SogA and its derivative point mutants in both wild-type and *sogA* null cells. Overexpression of SogA and SogA 2Ala had a negative impact in the chemotaxis phenotype of wild type and *sogA* null cells. Directionality and speed were even further decreased and the direction change further increased than the values of *sogA* null cells when either SogA or SogA 2Ala were over produced.

Figure 8 shows images captured from the chemotaxis videos of Ax2 (wild-type), *gxcGG*-, and *sogA*- null cells. These pictures are taken 5 minutes apart and show the behavior and appearance of the cells during chemotaxis. The shape of *gxcGG* null cells is similar to wild-type but more elongated. The *sogA* null cells are also elongated and send out many more pseudopods compared to wild-type.

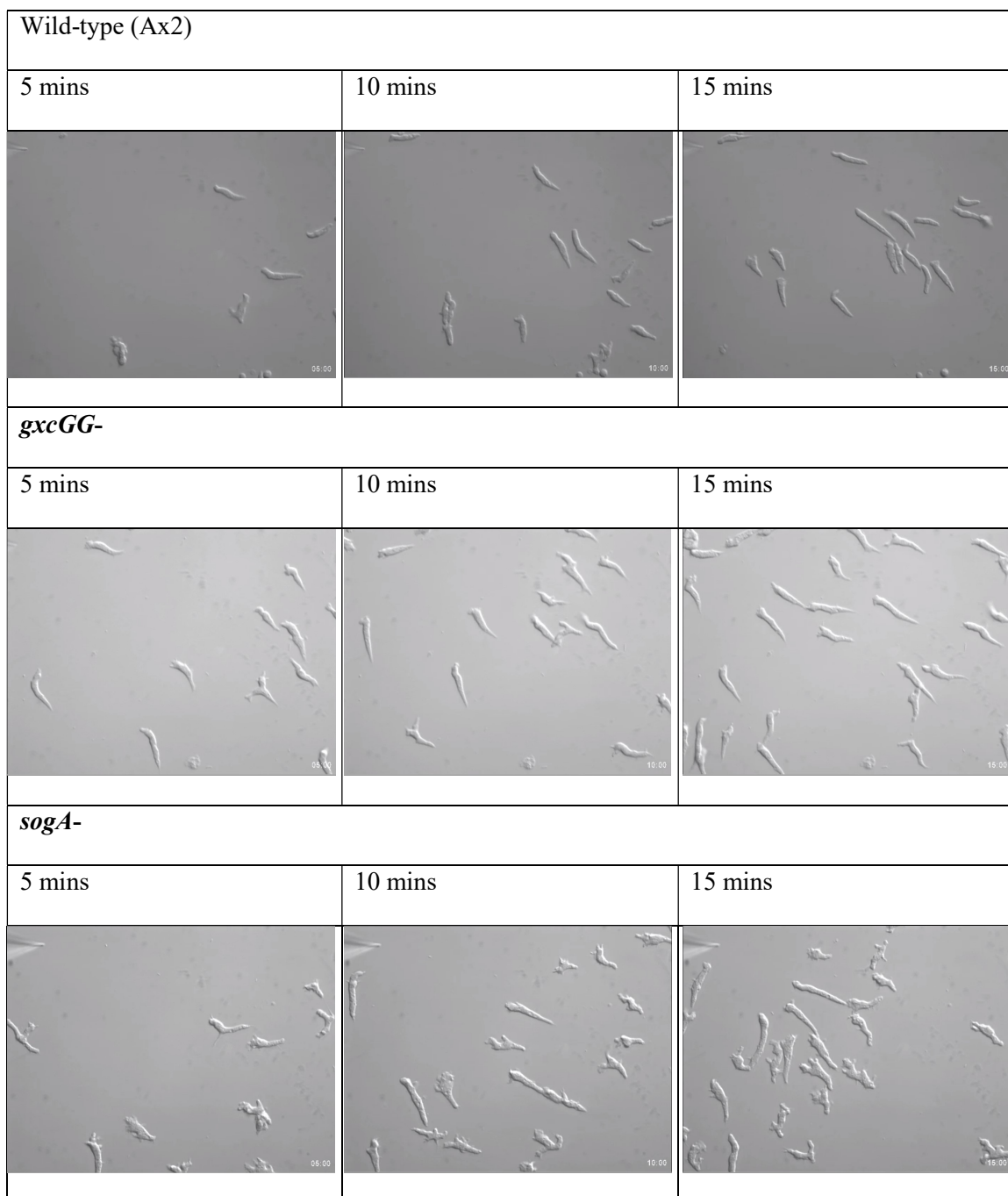


Figure 8: Images of wild-type cells compared with knockouts. Needle releasing cAMP chemoattractant is placed in the top left corner of each screen. The figure depicts cells chemotaxing towards the chemoattractant source at time point 5, 10, and 15 minutes.

Developmental assays for wild-type, *gxcGG* and *sogA* null cells.

Developmental assays were performed to further characterize the effects of knockouts and over-expression of *gxcGG* and *sogA* on *Dictyostelium* life cycle. Wild-type, *gxcGG*, and *sogA* null cells were starved on non-nutrient agar plates to study their development in response to starvation. Cells were plated on top of the agar and monitored every 3 to 4 hours under the scope to evaluate aggregation starting at 9 hours up to the formation of the fruiting body by the wild-type cells, usually around 24 hours.

Upon starvation, *Dictyostelium* wild-type cells aggregate together starting at 9 hours, and continue to differentiate into a base, stalk and a spherical spore head of a fruiting body that will be completed after 24 hours (Figure 9). At time point 9 hours, *gxcGG* had not begun to aggregate together. At time point 24 hours, *gxcGG* developed the stalk but the fruiting body still had an elongated spore head (Figure 9). This suggests that *gxcGG* may require more time to form a full fruiting body compared to the wild-type cells. *sogA* cells also had developmental defects compared to that of wild-type cells. *sogA* cells resulted in earlier *Dictyostelium* aggregation and mounds at 9 hours compared to wild-type. *sogA* also resulted in fruiting bodies with smaller spore heads at 24 hours (Figure 10).

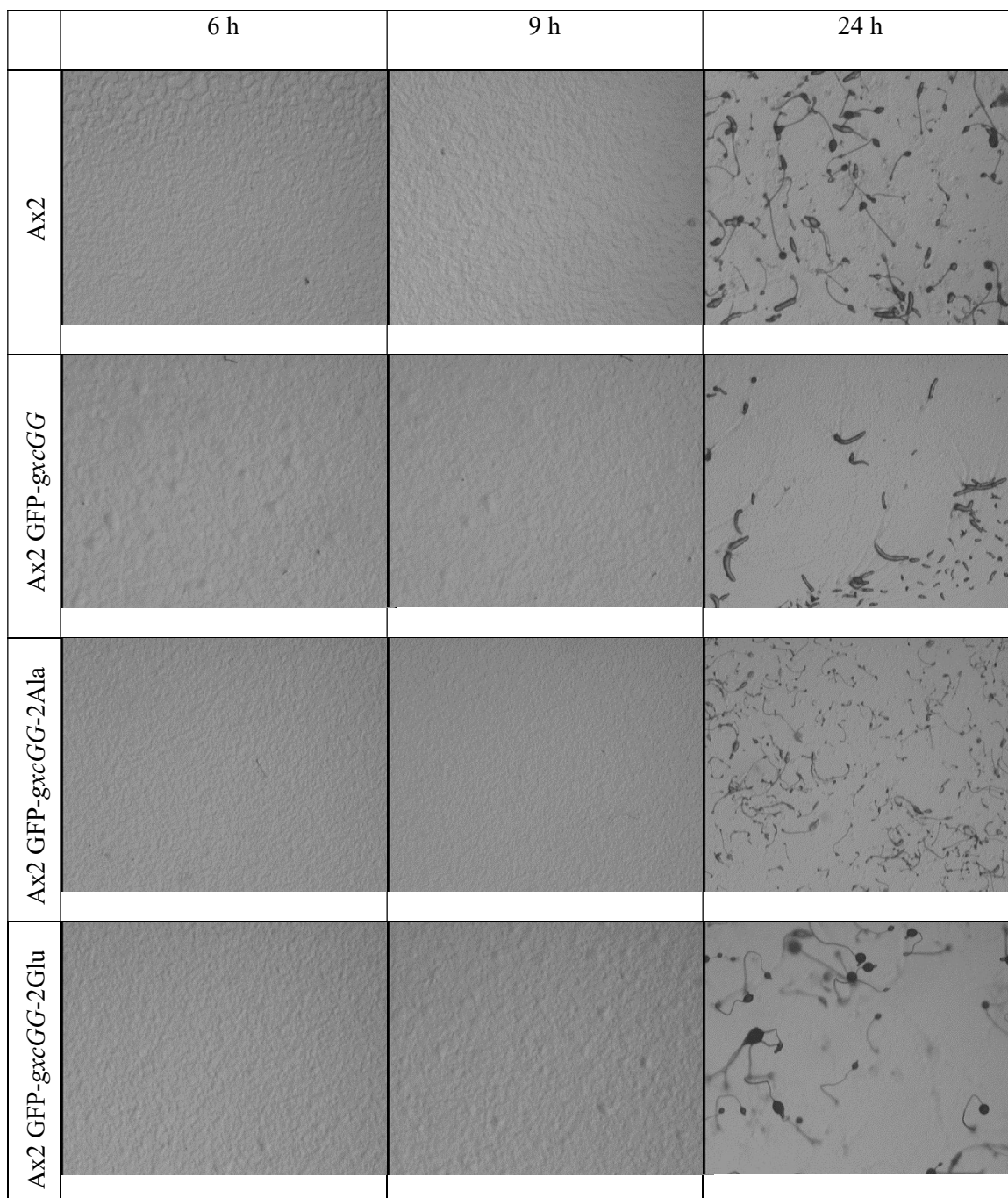


Figure 9: Developmental data for Ax2 with *gxcGG* overexpression. Representative time points of development pictures taken at 6, 9 and 24 hours of wild-type cells compared to over-expression of GFP-GxcGG, GFP-GxcGG-2Ala and GFP-GxcGG-2Glu in Ax2 (wild-type) cell lines.

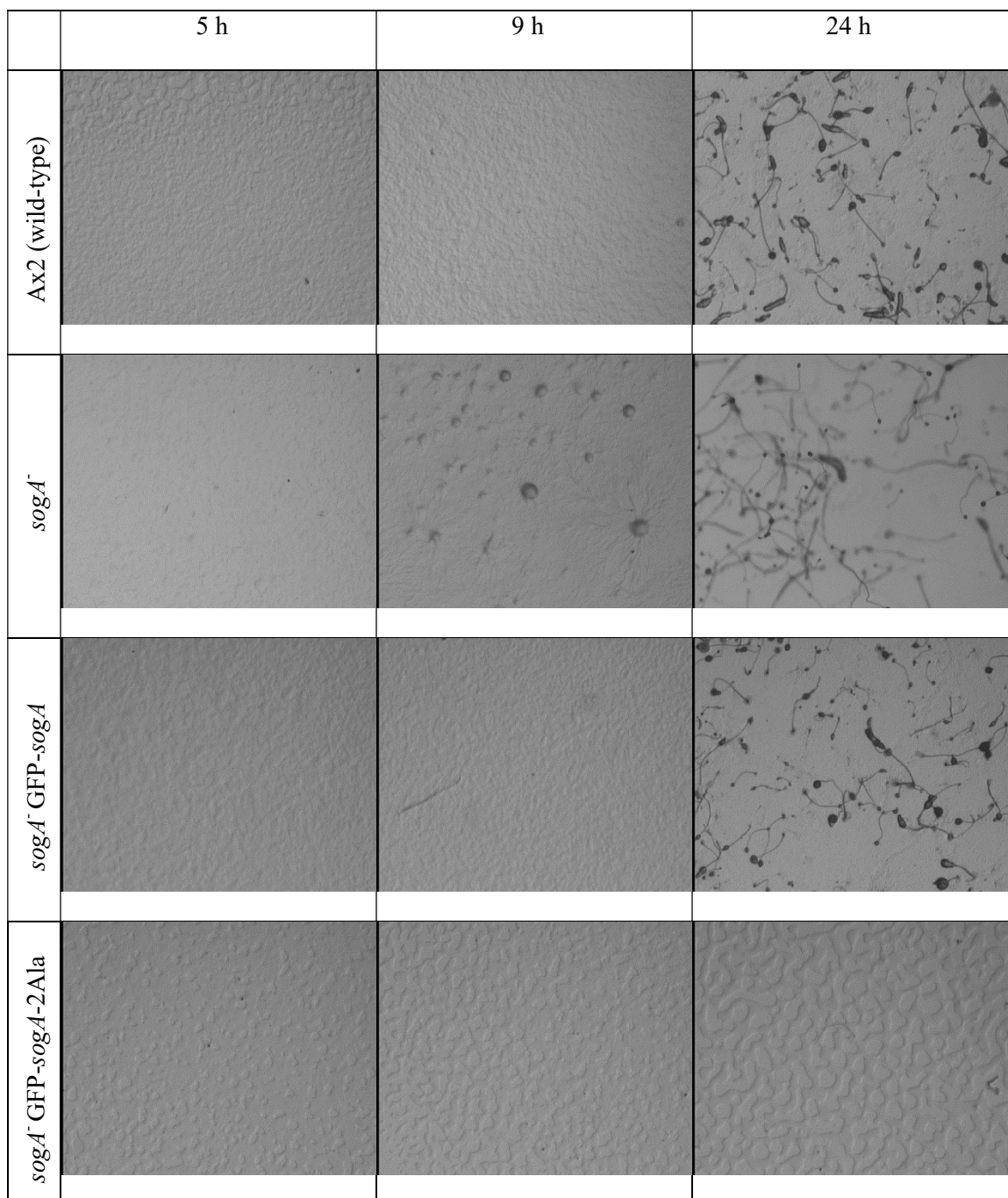


Figure 10: Developmental data for *sogA*⁻ cells with *sogA* and its derivatives. Development pictures taken at 5, 9, and 24 hours of *sogA* null cells compared to complement of *sogA*⁻ with GFP-*sogA* and GFP-*sogA*-2Ala

GxcGG over-expression in *gxcGG*⁻ (*gxcGG*⁻ GFP-*gxcGG*) caused an even more delayed development than *gxcGG*⁻. At 9 hours, *gxcGG*⁻ cells overexpressed with GxcGG did not show evidence of aggregation and at 24 hours were still in slug form with some slugs just beginning to form fruiting bodies (Figure 11). At 24 hours post-starvation, *gxcGG* 2Ala over-expression in *gxcGG*⁻ also only showed the slug form without any fruiting bodies (Figure 11). On the other hand, in *gxcGG*⁻ GFP-*gxcGG* 2Glu cells, the mutant pre-phosphorylated form of GxcGG was able to complement the development defect and the fruiting bodies were well-developed at 24 hours, similar to wild-type (Figure 11).

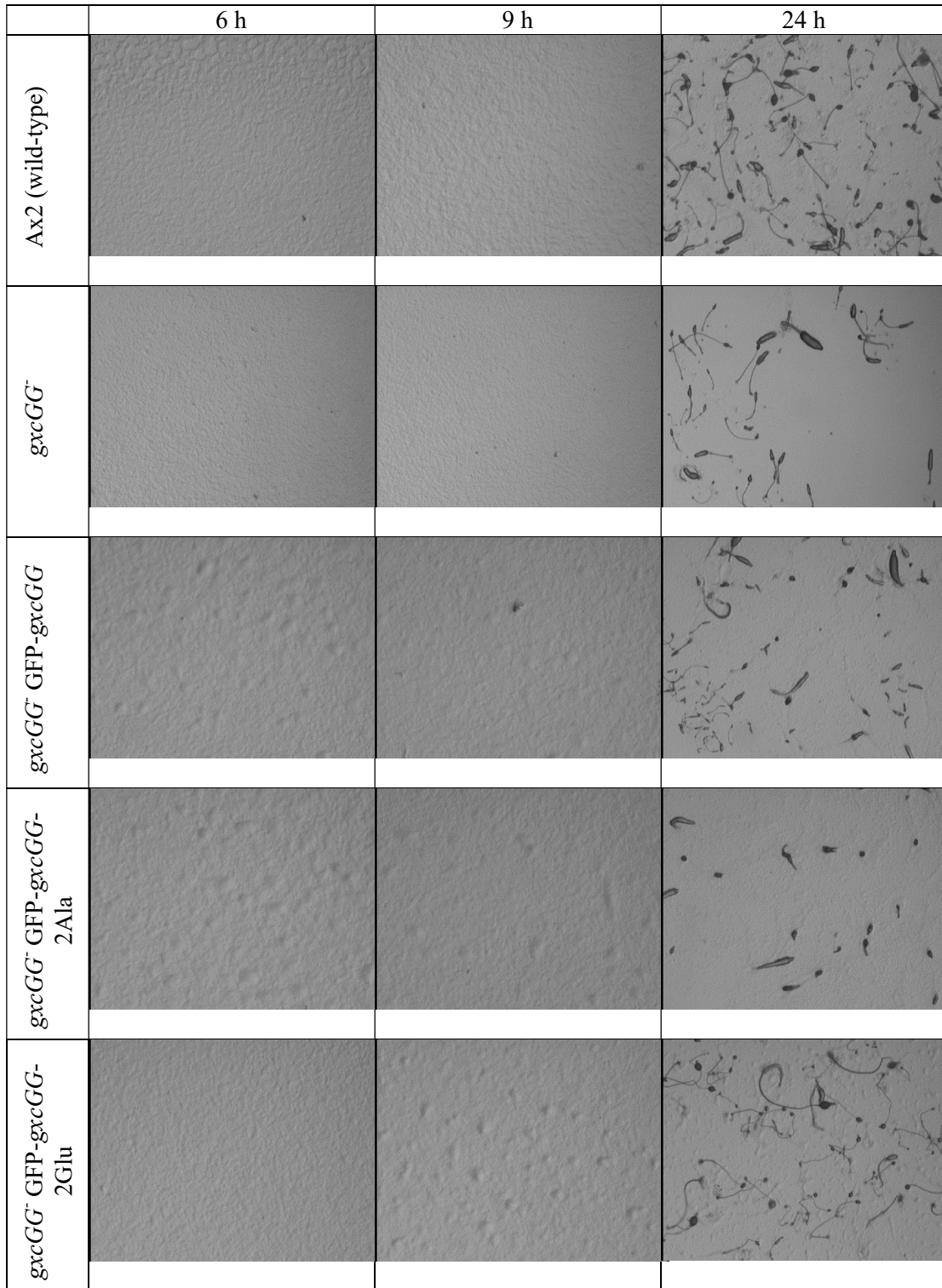


Figure 11: Developmental date for *gxcGG* null cell lines with over-expression of *gxcGG* and its mutant derivatives. Development pictures taken at 6, 9, and 24 hours of *gxcGG* null cells compared to complement of *gxcGG*⁻ with GFP-GxcGG, GFP-GxcGG-2Ala, and GFP-GxcGG-2Glu.

Over-expression of *gxcGG* in wild-type cells (Ax2 GFP-*gxcGG*) also resulted in delayed development at 9 and 24 hours. Aggregation was not captured at time 9 hours. There were no fruiting bodies and only various sized slug forms of *Dictyostelium*. In addition, at 24 hours, cells aggregated into the finger form (the development stage before the slug stage) (Figure 9). Additionally, Ax2 GFP-*gxcGG* 2Ala yielded small sized fruiting bodies compared with wild-type (Figure 9), whereas Ax2 GFP-*gxcGG* 2Glu cells resulted in well-developed fruiting bodies at 24 hours (Figure 9).

sogA overexpression in *sogA*⁻ cells (*sogA*⁻GFP-*sogA*) restores the knockout phenotype. By 9 hours, there is minimal evidence of aggregation of *sogA*⁻GFP-*sogA* seen by the slight clumping of the cells compared with time 5 hours. By 24 hours, complement of *sogA* caused fruiting bodies similar to wild-type (Figure 10). However at 9 hours, *sogA*⁻GFP-*sogA* 2Ala showed cells relatively aggregated together, but did not yield cells in the streaming phase or mounds (Figure 10). Over the 24 hour development phase, the *sogA*-2Ala overexpression in *sogA*⁻ cells gathered together but stayed flat along the development plate (Figure 10). Due to the non-viability of the cells, the *sogA*-2Asp overexpression in *sogA*⁻ was not available for the development assay.

Over-expression of *sogA*, *sogA*-2Ala, and *sogA*-2Asp in wild-type cells also resulted in fruiting bodies comparable to wild-type at 24 hours (Figure 12).

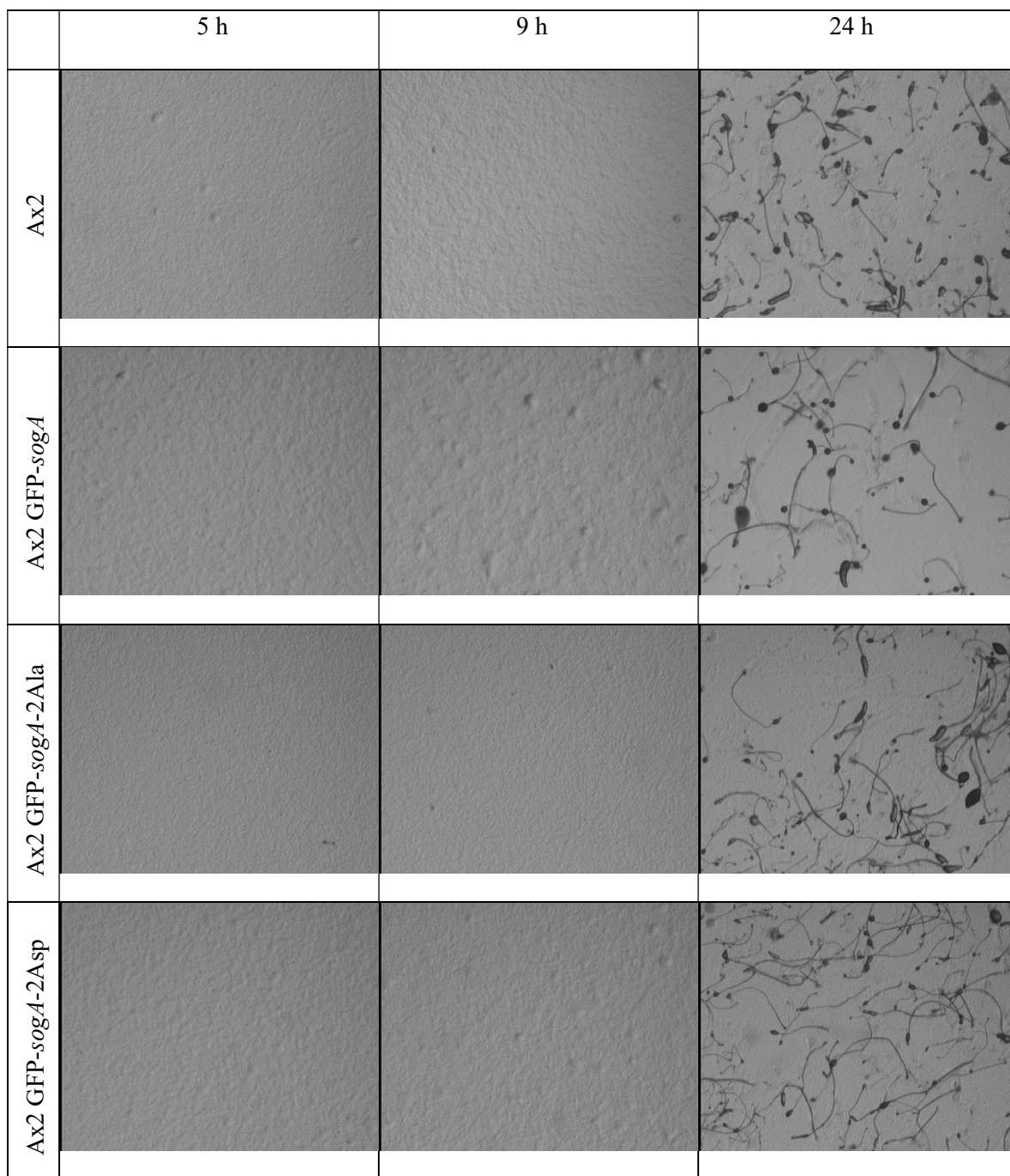


Figure 12: Developmental data for Ax2 with *sogA* overexpression. Development pictures taken at 5, 9, and 24 hours of wild-type cells compared to over-expression of GFP-SogA, GFP-SogA-2Ala, and GFP-SogA-2Asp in Ax2 (wild-type) cell lines.

Confocal analyses of GFP-GxcGG and GFP-SogA localization in vegetative and developed wild-type and their respective null cells

GFP tagged GxcGG and SogA protein localization was analyzed in wild-type and their respective null cells. Vegetative and chemotaxis competent (developed) cells were placed on glass slides containing a non-nutrient buffer and allowed to adhere to the surface for 20 minutes. For random motility assays using vegetative cells, localization of GFP-GxcGG and GFP-SogA was monitored by taking pictures every 6 sec for 30 minutes. Using developed cells, uniform cAMP stimulation and chemotaxis assays were performed. For uniform cAMP stimulation assays, 200 μ l of a 150 μ M cAMP solution was injected onto the plate (containing 3ml of Na/K phosphate buffer) to stimulate the cells globally. The subsequent cortex translocation of the GFP fusion proteins was digitally recorded by taking pictures every 1 sec for 60 sec. For chemotaxis, a needle containing 10 μ M of cAMP was placed near the cells, and cell migration toward the needle was monitored by taking pictures every 6 sec for 15 to 30 minutes.

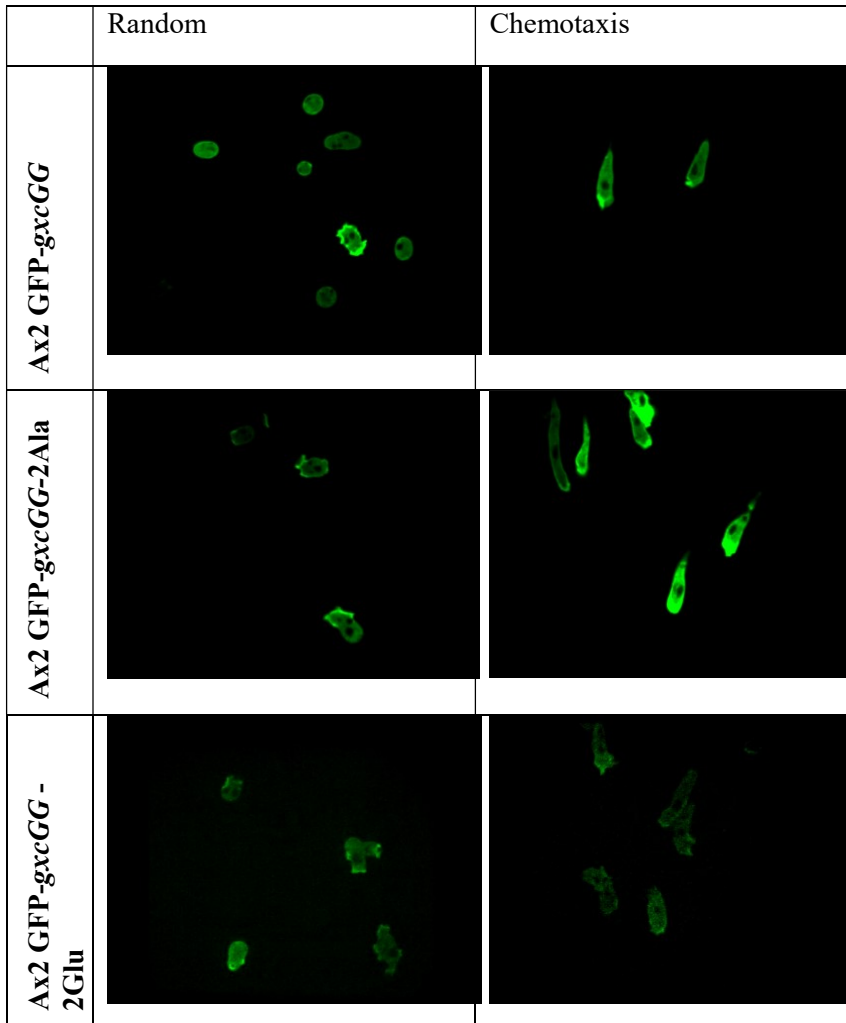


Figure 13: GFP localization data for GxcGG overexpression in wild-type cells in random and chemotaxis *in vivo* assays. The bright green color indicates higher concentrations of GFP-tagged protein. In the chemotaxis photos, the cells are chemotaxing towards the cAMP source at the bottom midline position. There is a clear increased concentration of GFP-tagged protein in the leading edges and protrusions made during random and chemotaxis movement.

In vegetative cells, the analysis of protein localization during random movement shows that GxcGG and its mutant derivatives localize at the cell's protrusions during random movement (Figures 13 and 14). In contrast, the protein localization of SogA and its derivatives show that the protein does localize to the protrusions, however much of the protein still remains in the cytosol (Figure 15).

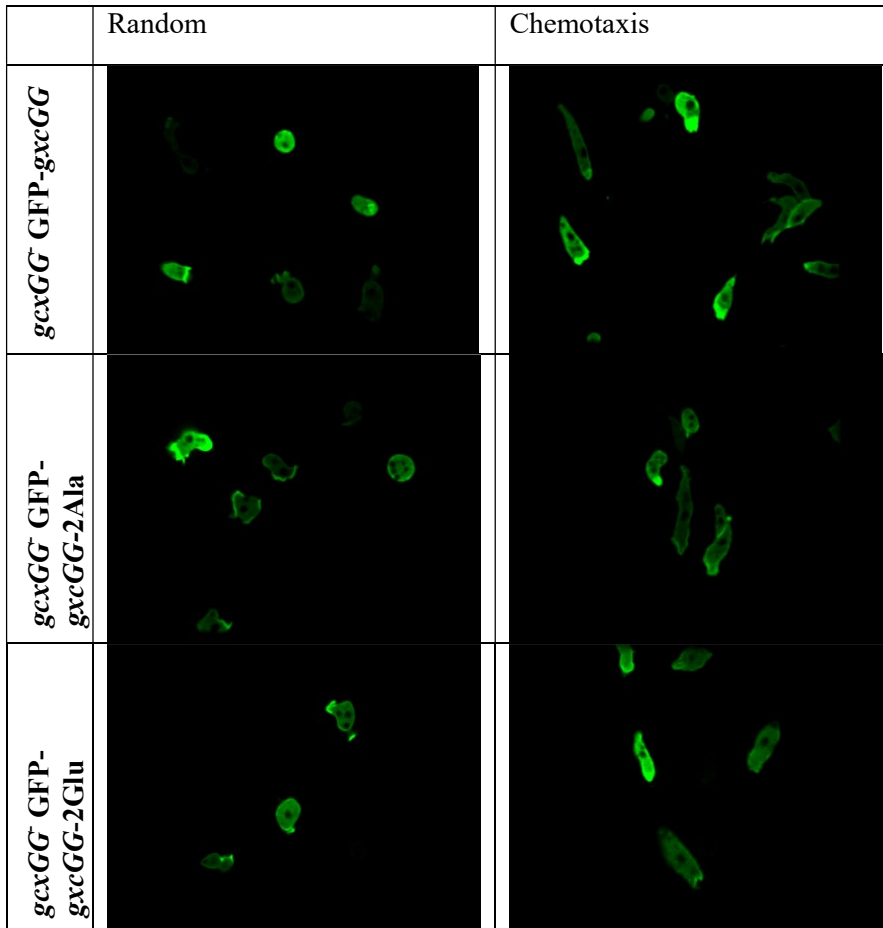


Figure 14: GFP localization data for GxcGG protein derivatives in *gxcGG* in random and chemotaxis *in vivo* assays. The bright green color indicates higher concentrations of GFP-tagged protein. In the chemotaxis photos, the cells are chemotaxing towards the cAMP source at the bottom midline position. There is a clear increased concentration of GFP-tagged protein in the leading edges and protrusions made during random and chemotaxis movement.

In developed cells, both GFP-GxcGG and GFP-SogA (as well as their mutant derivatives) show protein localization to the leading edge during chemotaxis (Figures 13 and 14). This localization suggests that both proteins may be components of the cAMP-signaling pathway. GFP-GxcGG proteins and its derivatives however, have a more pronounced concentration of GFP tagged protein at the leading edge with a decrease in protein concentration in the cytoplasm (Figures 13 and 14), whereas GFP-SogA and its derivatives translocate to the membrane, but continues to have a confluence of GFP-tagged protein within the cytoplasm (Figure 15).

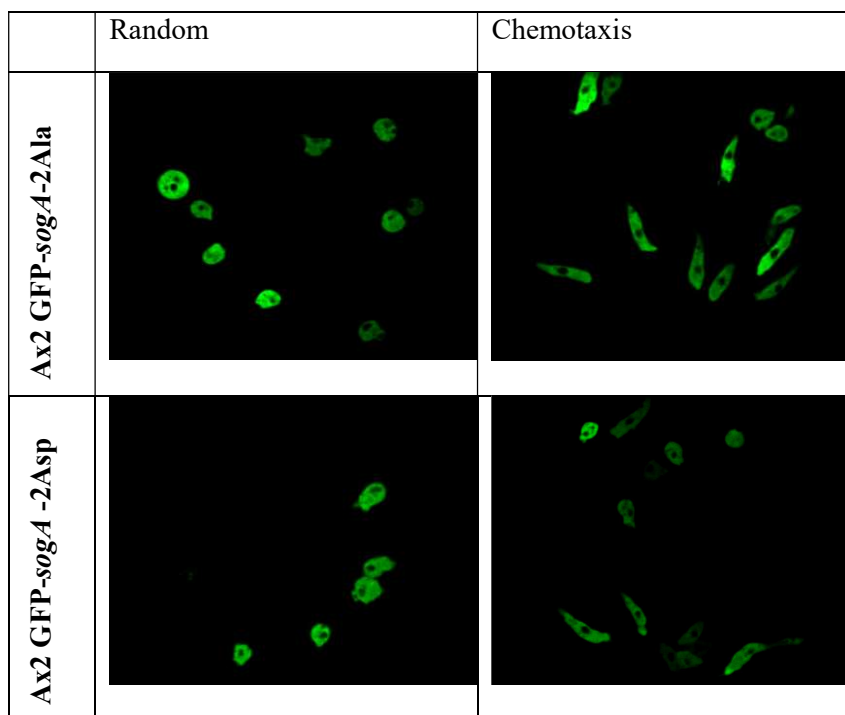


Figure 15: GFP localization data for SogA overexpression in random and chemotaxis *in vivo* assays. The bright green color indicates higher concentrations of GFP-tagged protein. In the chemotaxis photos, the cells are chemotaxing towards the cAMP source at the bottom midline position. There is a lack of a clear leading edge during random and chemotaxis movement.

In response to uniform cAMP stimulation, GFP-GxcGG and its mutant derivatives rapidly translocate to the plasma membrane as a result of global stimulation by cAMP (Figure 16). The *gxcGG* native and derivative mutant proteins have a clear translocation to the membrane in both over-expression and complementation cell lines (Figure 16). Before cAMP stimulation, GFP-GxcGG is in the cytoplasm (Figure 16). Shortly after cAMP stimulation, the localization of GFP-GxcGG to the cell cortex peaks around 7-10 seconds (Figure 16). This is clearly shown by the bright green rim around the cell cortex and the darkening of the cytoplasm.

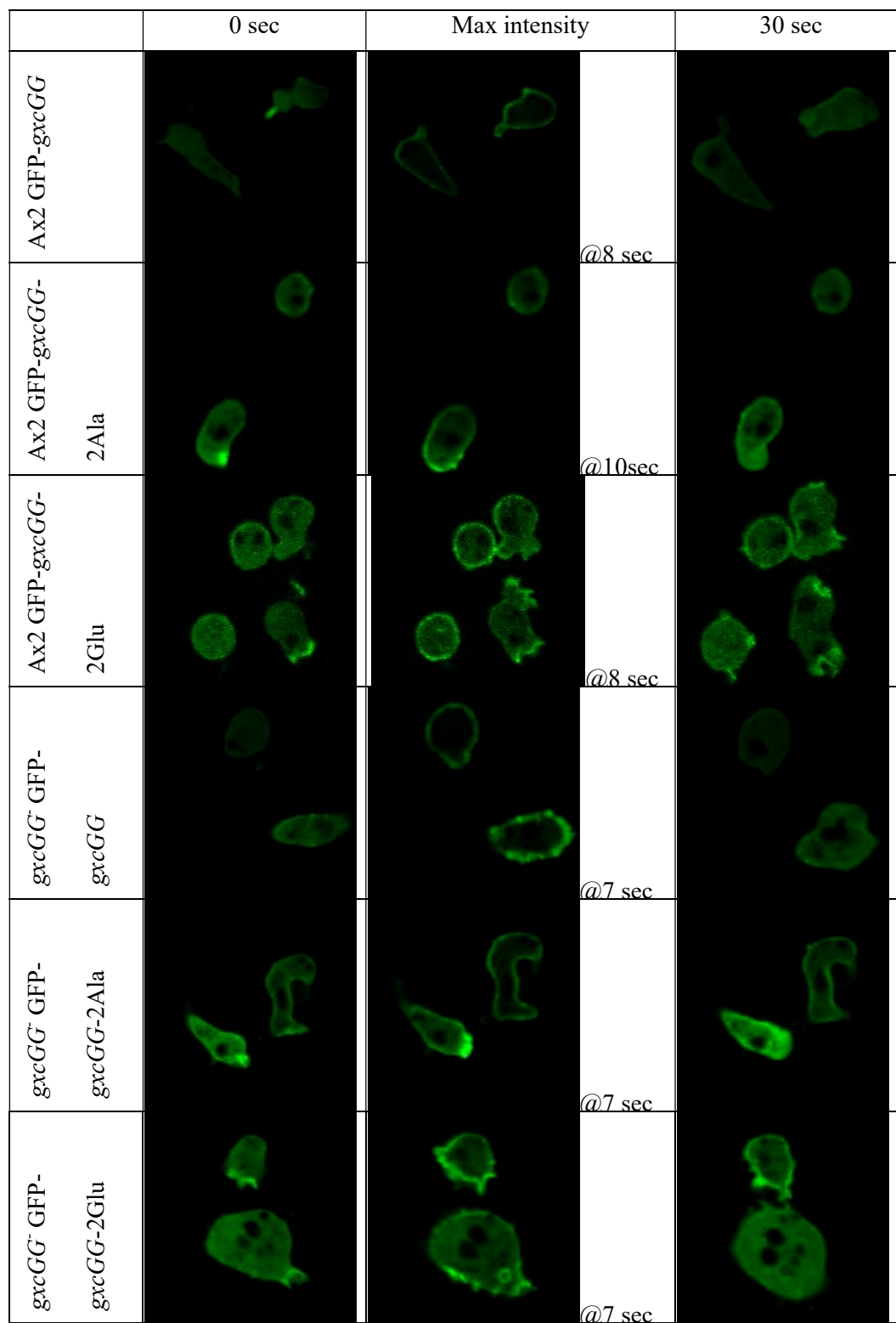


Figure 16: Global Stimulation data for overexpression of GxcGG. Cells were stimulated with cAMP at time point 0 seconds. At time of maximum intensity, the green rim that represents the GFP-tagged protein localization concentrates at the cytoskeleton.

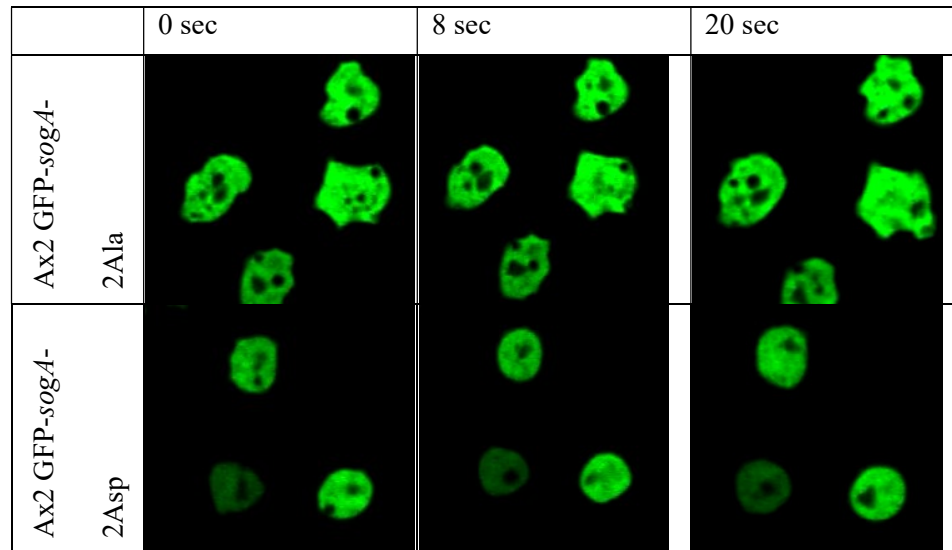


Figure 17: Global Stimulation data for overexpression of SogA-2Ala and 2Glu derivatives. Cells were stimulated with cAMP at time point 0 seconds. At 8 seconds after cAMP stimulation, the GFP-tagged SogA proteins did not show localization to the cytoskeleton.

In a sharp contrast to the GxcGG membrane localization, SogA and its derivatives hardly translocated to the membrane in response to uniform cAMP stimulation. Shown in Figure 17, the GFP-SogA fusion proteins stayed in the cytoplasm after global stimulation. In contrast, during chemotaxis, GFP-SogA translocated to the leading edge although not as tightly localized to the edge of the cytoskeleton as GFP-GxcGG proteins and its derivatives (Figure 15).

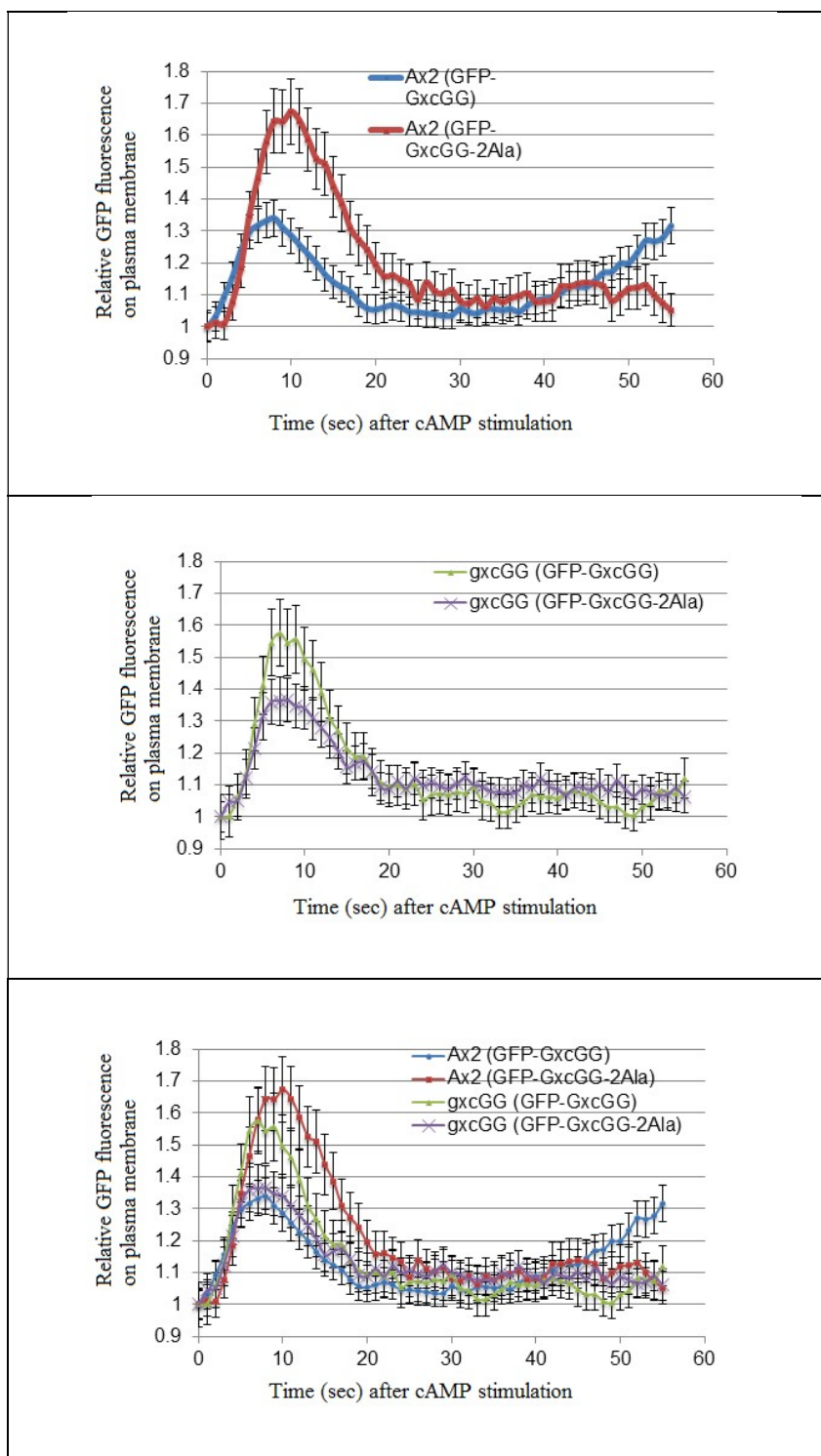


Figure 18: Global Stimulation of gxcGG strains in Ax2 and gxcGG⁻ cells. Graph shows the relative GFP fluorescence against time in seconds after cAMP stimulation. Ax2 overexpressed with GFP-GxcGG 2Ala) had the highest relative GFP fluorescence at approximately 1.7 relative fluorescence.

III. DISCUSSION

Identification of direct substrates of *Dictyostelium* GSK3 through phosphoproteomics

Through the use of phosphoproteomics and bioinformatics of wild-type and *gskA* null cells, potential substrates of GSK3 were identified by the presence of the S/TPXXS/TP consensus site and its response to phosphorylation in both strains. Under our experimental conditions, phosphoproteomics postulated GxcGG and SogA proteins, as GSK3 direct substrates in vivo, and identified Thre753 and Ser757 on GxcGG and Ser565 and Ser569 on SogA as the potential GskA (*Dictyostelium* GSK3) phosphorylation sites. Thre753, Ser757, Ser565 and Ser569 were phosphorylated in wild-type cells but not in *gskA*⁻ cells. The detection of other GxcGG and SogA peptides guaranteed the presence of the proteins in the proteome of both strain, suggesting that the lack of phosphorylation in the *gskA*⁻ cells might be due to the lack of GskA rather than GxcGG or SogA being absent in the *gskA*⁻ cells. Similar phosphosites have been detected in previous phosphoproteomics experiments carry out in wild-type cells in response to the chemoattractant cAMP, strongly suggesting that these sites are phosphorylated in vivo, and presumably regulated by cAMP stimulation (Charest et al., 2012). This proves the sensitivity of the phosphoproteomic assay. This assay was also vital to other studies by the Firtel lab to identify the first GSK3 substrate, Daydreamer (Kölsch et al., 2013). Therefore, our phosphoproteomic assay was useful for the identification of transient phosphorylations in response to chemoattractant stimulation. Our preliminary proteomics analysis postulated GxcGG and SogA as potential GskA direct substrates in chemotaxis in *Dictyostelium discoideum*.

SogA: A GSK3 direct substrate

SogA is a substrate of GSK3 as shown in the initial phosphoproteomic assays. According to phosphoproteomics, SogA increased in phosphorylation in wild-type cells, in response to the chemoattractant, whereas the same phosphorylation did not happen in *gskA* cells, under our experimental conditions. Orthologs of SogA exist in various species including *Homo sapiens*, *Dictyostelium purpureum*, *Saccharomyces cerevisiae* and *Drosophila melanogaster* according to sequencing studies with 29, 68, 30 and 27 % of identity. A kelch repeat-containing protein 2 sequence is also identified in *sogA* through proteomic analysis. Although little is known about the function of kelch repeats, the multiple kelch repeats create a β -propeller structure involved in protein-protein interaction. Due to the presence of the kelch repeats, there is potential for SogA to regulate the cytoskeleton of the cells (Philips, 1998). Bioinformatics studies revealed that the kelch domain architecture is well conserved in *H. sapiens* with 72% of the kelch-repeat superfamily coming from the metazoan animal BTB/kelch type proteins (Prag et al., 2003). The fact that kelch repeat containing proteins are conserved in higher eukaryotes as well as GSK3, brought my attention to this protein in *Dictyostelium*. An example of a Kelch containing protein is Keap1. In mice, Keap1, a Kelch containing gene that encodes an adaptor and substrate receptor for Cul3-Rbx1/Roc1 ubiquitin ligase, has a substrate receptor Nrf2 (Chowdhry et al., 2013). Nrf2 is found to contain a β -TrCP motif that is modulated by GSK3. Regulation of Nrf2 may reveal more information on how to manage tumors that contain Keap1 mutations (Chowdhry et al., 2013).

The *in vitro* phosphorylation assay results revealed that GSK3 is accountable for the phosphorylation of *sogA in vitro*, and specifically, at the residue identified with proteomics, Ser⁵⁶⁵. This conclusion is further supported in the chemotaxis results which suggest that *sogA* has a role in cell movement, cell shape and direction change. Interestingly, *sogA* play a role in development as well as chemotaxis. The *sogA* null cells affected *Dictyostelium* development by causing earlier

cell aggregation and smaller fruiting body spore heads. Over-expression of SogA and its protein derivatives yielded similar results as wild-type development. As expected, expression of SogA-2Ala did not return wild-type phenotype and instead, resulted in lack of fruiting bodies even with cell aggregation. According to our fluorescence visualization data on global stimulation and random and chemotaxis movement, *sogA* does not translocate to the cell membrane in response to uniform cAMP stimulation but it does localize at the leading edge of chemotaxing cells, suggesting that perhaps SogA localization depends on cell polarization. Interestingly, *sogA* knockout causes decreased chemotaxis and development function. This suggests that *sogA* plays a role in signal transduction related to cell movement and aggregation, and it might be regulated by GSK3 phosphorylation. In order to further assess the function of *sogA* in *Dictyostelium* chemotaxis, additional biochemical assays including the study of the cytoskeleton (F-actin polymerization and myosin II assembly), and activation of Ras, AKT/PKB and Rap1 signaling pathways will be study in detail

GxcGG: A GSK3 direct substrate

Phosphoproteomic assays revealed *gxcGG* as a potential GSK3 substrate due the increased phosphorylation of the protein in wild-type cells in response to cAMP stimulation. For this reason, *gxcGG* was selected as one of the candidate genes going forward in this project. GxcGG is a protein from the family of guanine exchange factors for rac. This protein has not been previously studied but other RacGEF proteins such as GxcC are known to play a role in the regulation of development, and they also contain a PH domain. According to the DictyBase (JGI/Baylor Sequencing Project), currently the only other ortholog of GxcGG exists in *Dictyostelium purpureum*. After investigation of *gxcGG* as a candidate substrate of GSK3, the protein *gxcGG* was found to be phosphorylated by GSK3 *in vitro*. However, due to the phosphorylation of the protein containing the mutated GSK3 sites that we identified with

proteomics, we cannot conclude whether that particular site is being phosphorylated *in vitro*. Due to the presence of multiple potential GSK3 sites in GxcGG, we think we are having other sites being phosphorylated, specifically or not, *in vitro*. In addition, the recombinant human GSK3 beta used for the experiment may have had a different specificity to the *Dictyostelium* GSK3.

Chemotaxis and development data showed that *gxcGG* has a significant role in the proper response of *Dictyostelium* movement. The knockout strains showed noteworthy decrease in speed, directionality and elongated shape changes from wild-type. This slower chemotaxis also caused expected development delays such as slug-formed cells and incomplete fruiting bodies given the same amount of time wild-type cells need to form complete fruiting bodies.

GxcGG contains a pleckstrin homology (PH) domain, which is associated with proteins that have a role in cell signaling with the cytoskeleton. Proteins may be recruited to the cytoskeleton through interactions between phosphatidylinositol lipids within cell membranes and the protein's PH domain. Previous studies have shown that knockouts of other PH domain containing proteins exhibit defects in leading edge actin polymerization and chemotaxis defects (Firtel et al., 2001). Phenotypes of previously studied PH domain containing mutants suggest that these proteins may regulate F-actin localization at the cell leading edge in response to chemoattractants. Therefore, the presence of PH domains in *gxcGG* leads to the assumption that GxcGG protein would be localized to the leading edge responses to cAMP. Indeed, the fluorescence localization assays revealed that *gxcGG* is strongly associated with cell movement and structure. In chemotaxis assays of GFP-tagged GxcGG, the protein clearly concentrated at the leading edge. Even in cells under no cAMP stimulation displayed the concentration of protein brightest where the cell membrane was changing and forming pseudopods. Furthermore, GFP-GxcGG quickly associated with all edges of the cell when uniformly stimulated with cAMP. This highly suggests GxcGG as a protein that regulates cell movement and membrane structure. This protein will be further tested by actin-myosin biochemical assays.

The chemotaxis speed of *gxcGG*⁻ and *sogA*⁻ is 8.03 ± 1.39 $\mu\text{m}/\text{min}$ and 8.89 ± 1.83 $\mu\text{m}/\text{min}$, respectively. The chemotaxis speed of *gskA*⁻ is 6.12 ± 1.95 $\mu\text{m}/\text{min}$ (Kölsch et al., 2013). Although *gxcGG*⁻ and *sogA*⁻ cell lines have clear chemotaxis and development defects, they are not as severe as the ones observed for GSK3. This comparison suggests that maybe more substrates of GSK3 remain to be identified. It also possible that the combination of Daydreamer, SogA, and GxcGG proteins functions under the control of GSK3 and the combination is essential for proper chemotaxis. The current hypothesis is that the severe defective phenotypes of GSK3 are due to the sum of multiple proteins that fail to be regulated by GSK3 in the *gskA* null cell lines.

IV. MATERIALS AND METHODS

D. *dicoideum* growth and differentiation.

D. discoideum cells were cultured axenically at 21°C in HL5 medium containing 1 % (v/v) of antibiotic:antimycotic solution (Gemini Bio-Products). Cells used and created in this study are listed in Table 1. Cells carrying expression constructs were maintained in the same medium containing 10-20 $\mu\text{g/ml}$ G418. To obtain developmentally competent cells capable of responding to cAMP as a chemoattractant, log-phase vegetative cells were harvested by low-speed centrifugation (1500 rpm for 3 minutes), washed twice and resuspended at a density 5×10^6 cells/ml with 12 mM Na/K phosphate buffer, pH 6.2, and pulsed with 7.5 μM cAMP solution for 5.5 h at 6-min intervals. Cells were then washed and resuspended in 12 mM Na/K phosphate buffer.

Protein domain prediction.

Domain prediction models were created using Prosite-ExPasy, Pfam, and SMART databases. GxcGG and SogA protein sequences were obtained from the Dictydatabase (<http://dictybase.org/>).

Plasmids and Cell Lines.

Potential substrates for GSK3 are listed in Table 1. The genomic and or cDNA of potential substrates for GSK3 were cloned in pBlueScript SK- and into a modified EXP-4(+) vector which added either a GFP tag (356 amino acids) or a T7 tag (MASMTGGQMG) to the N terminus of the protein. The desired and clean PCR products were digested routinely with SpeI/XhoI and ligated into the vector digested with the same enzymes. Cloning of the correct sequence was verified by sequencing. *gskA* null cells were transformed with the purified plasmids. For directed cell mutagenesis, genes cloned in pBlueScript SK- were used along with the primers containing the desired point mutations in the GSK3 site to generate the 2Ala, 2 Asp or 2 Glu mutations.

Electroporation.

Transformation was done in E buffer (12 mM Na/K phosphate, 50 mM sucrose, pH 6.1) by electroporation of 20 µg DNA per 8×10^6 cells using a Bio-Rad Gene Pulser II set at 1 kV and 3 µF. After overnight recovery in HL5 in a 100-mm Petri dish, cells were selected in the appropriate antibiotic for transformants.

Immunoprecipitation of the potential substrates.

Cells were grown in HL-5 medium supplemented with G418 on plates to exponential growth phase. Cells density was count using a hemacytometer and 5×10^7 cells/ml samples were harvested by centrifuging 3 min 1500 rpm. Cells were lysed (lysis buffer) for 10 minutes at 4°C vortexing every 2 minutes. Then, samples were centrifuged at 12500 rpm at 4°C for 10 minutes and the supernatant was incubated with 25 µl of T7 Tag Antibody Agarose (Novagen #69026) for 2 hours at 4°C. Beads were washed three times with 1x lysis buffer and one eventually with 1x kinase buffer. Beads were kept O/N at 4 °C prior to the kinase assay.

GSK3 Kinase assay.

To determine whether candidate proteins GxcGG and SogA are phosphorylated by GSK3 *in vitro*, a kinase assay was carried out in the presence of immunoprecipitated candidate protein and P32 gamma ATP. Wild type cells with and without overexpressing T7-GxcGG or T7-SogA were grown on plates to exponential growth phase. Cells density was count using a hemacytometer and 5×10^7 cells/ml samples were harvested by centrifuging 3 min 1500 rpm. Cells were lysed (lysis buffer) for 10 minutes at 4°C vortexing every 2 min. Then, samples were spun at 12500 rpm at 4°C for 10 min and the supernatant was rocked with 25 µl of T7 Tag Antibody Agarose (Novagen #69026) for 2 hours at 4°C. After that, beads were washed three times with 1x lysis buffer and one eventually with 1x kinase buffer. Beads were kept O/N at 4 °C prior to the kinase assay. Then 20 µl of a P32 gamma ATP cocktail solution (250 µM cold ATP, 0.16 µCi hot ATP, 1 x Kinase Buffer {5 mM MOPS pH 7.2, 2.5 mM Beta-Glycerolphosphate, 5

mM MgCl₂, 1 mM EGTA, 0.4 mM EDTA, 0.05 mM DTT, 20 µg/ml BSA}) was added to the immunoprecipitated samples. After incubation for 30 min at room temperature, the kinase reaction was stopped by adding 40 µl of 2x SDS loading buffer. Samples were boiled four minutes and placed on ice until loaded in a SDS-PAGE gel and transfer to nitrocellulose membranes. The membranes were O/N exposed to HYBLOT CL Premium Autoradiography film for autoradiography (Denville Scientific INC).

Electrophoresis and Immunoblotting.

SDS-PAGE was performed by standard procedures using Tris glycine gels. Gels were stained with Coomassie Blue or immunoblotted. Immunoblotting was performed as described previously (Towbin et al., 1979). Cell lysates were subjected to 10% SDS-PAGE analysis and transferred to Immuno-Blot PVDF membrane. The membrane was blotted with polyclonal antibodies. Detection was performed by chemiluminescence using a donkey anti-rabbit antibody and GE Healthcare ECL Western blotting detection reagents (Amersham ECL Plus GE Healthcare Life Sciences).

Chemotaxis assays.

Chemotaxis analysis was performed as described previously (Park *et al.*, 2004; Sasaki *et al.*, 2004) and analyzed using DIAS software (Wessels *et al.*, 1998). Differentiated cells were plated in Na/K phosphate buffer at a density of 5×10^4 cells/ml onto a plate with a hole covered by a 0.17 mm glass coverslip and allowed to adhere to the surface for 20 min. An Eppendorf Patchman micromanipulator with a glass capillary filled with 150 µM cAMP solution was brought into the field of view of an inverted microscope (XXXXXX; Nikon) with a 40x NA 0.4 objective lens. The response of the cells was recorded by time-lapse video. Experiments were performed at least three times on different days, always including a wild-type control strain in the analyses.

GFP Localization assays

GFP Localization analysis was performed and analyzed using DIAS software (Wessels et al.,1998). Differentiated cells were plated in Na/K phosphate buffer at a density of 5×10^4 cells/ml onto a plate with a hole covered by a 0.17 mm glass coverslip and allowed to adhere to the surface for 20 min. An Eppendorf Patchman micromanipulator with a glass capillary filled with 150 μ M cAMP solution was brought into the field of view of a microscope. The response of the cells was recorded by time-lapse video. Experiments were performed at least three times on different days, always including a wild-type control strain in the analyses.

Global Stimulation assays

Global Stimulation analysis was performed and analyzed using DIAS software (Wessels et al.,1998). Differentiated cells were plated in Na/K phosphate buffer at a density of 5×10^4 cells/ml onto a plate with a hole covered by a 0.17 mm glass coverslip and allowed to adhere to the surface for 20 min. 200 μ l of 150 μ M cAMP solution was injected into plate. The response of the cells was recorded by time-lapse video. Experiments were performed at least three times on different days, always including a wild-type control strain in the analyses.

Development assays.

Cells were harvested from plates at a log phase density, washed twice and concentrated to 3×10^7 cells/ml in Na/K phosphate buffer. Serial dilutions of 30 μ l drops were placed on Na/K phosphate agar plates. Development was monitor during 24 hours at room temperature.

REFERENCES

- Amselem, G., Theves, M., Bae, A., Beta, C and Bodenschatz, E. (2012). Control parameter description of eukaryotic chemotaxis. *Physical Review Letters*. 109, 108103.
- Bonner, J.T. (1971). Aggregation and differentiation in the cellular slime molds. *Annual Review Microbiology*. 25, 75-92.
- Cai H, Huang CH, Devreotes PN, Iijima M. Analysis of chemotaxis in *Dictyostelium*. *Methods Mol Biol*. 2012;757:451-68.
- Charest, P.G., Shen, Z., Lakoduk, A., Sasaki, A.T., Briggs, S.P., and Firtel, R.A. (2010). A Ras signaling complex controls the RasC-TORC2 pathway and directed cell migration. *Developmental Cell*. 18. 737-749.
- Chowdhry, S, Y Zhang, M McMahon, C Sutherland, and A Cuadrado. "Nrf2 is controlled by two distinct β -TrCP recognition motifs in its Neh6 domain, one of which can be modulated by GSK-3 activity." *Oncogene* 32 (2013): 81-3765. Web. 16 Nov. 2014.
- Fiol, C.J., Haseman, J.H., Wang, Y.H., Roach, R.J., Roeske, R.W., Kowalczyk, M., and DePauli-Roach, A.A. (1988). Phosphoserine as a recognition determinant for glycogen synthase kinase-3: phosphorylation of a synthetic peptide based on the G-component of protein phosphatase-1. *Archives of Biochemistry and Biophysics*. 267. 797-802.
- Frame, S., and Cohen, P. (2001). GSK3 takes centre stage more than 20 years after its discovery. *Biochemistry*. 359. 1-16.
- Funamoto S, Milan K, Meili R, Firtel RA. Role of phosphatidylinositol 3' kinase and a downstream pleckstrin homology domain-containing protein in controlling chemotaxis in *dictyostelium*. *J Cell Biol*. 2001;153(4):795-810.
- Haastert, P.J.M., and Bosgraaf, L. (2009). The local cell curvature guides pseudopodia towards chemoattractants. *HFSP Journal*. 3. 282-286.
- Kim, D., and Haynes, C.L. (2012). Neutrophil chemotaxis within a competing gradient of chemoattractants. *Analytical Chemistry*. 84. 6070-8.
- Kim, L., Brzostowski, J., Majithia, A., Lee, N.S., McMains, V., and Kimmel, A.R. (2011). Combinatorial cell-specific regulation of GSK3 directs cell differentiation and polarity in *Dictyostelium*. *Development and Stem Cells*. 138. 421-30.
- Kölsch, V., Shen, Z., Lee, S., Lotfi, P., Chang, J., Charest, P.G., Romero, J.L., Jeon, T.J., Briggs, S.P., and Firtel, R.A. (2013). Daydreamer, a Ras/Rap1 effector and GSK-3 substrate, is important for directional sensing and cell motility. *Mol Biol Cell*. 24. 100-14.
- Lee, S., Comer, F.I., Sasaki, A., McLeod, I. X., Duong, Y., Okumura, K., Yates, J.R., Parent, C. A., Firtel, R.A. (2005). TOR complex 2 integrates cell movement during chemotaxis and signal relay in *Dictyostelium*. *Mol Biol Cell*. 16(10):4572-83.

- Lee, S., Firtel, R.A.. *Aggregation towards cAMP*. University of California, San Diego. *Dictybase Development*. Web. 28 Feb. 2016.
- Lee, S., Shen, Z., Robinson, D.N., Briggs, B., and Firtel, R.A. (2010). Involvement of the cytoskeleton in controlling leading-edge function during chemotaxis. *Molecular Biology of the Cell*. 21, 1810-1824.
- Leger, J., Kempf, M., Lee, G., and Brandt, R. (1997). Conversion of Serine to Aspartate Imitates Phosphorylation-induced Changes in the Structure and Function of Microtubule-associated Protein Tau. *The Journal of Biochemical Chemistry*. 272. 8441-46.
- Liu, L., Aerbajinai, W., Ahmed, S.M., Rodgers, G.P., Angers, S., and Parent, C.A. (2012). Radil controls neutrophil adhesion and motility through β 2-integrin activation. *Mol Bio Cell* [Epub ahead of print].
- Meili R, Firtel RA. Two poles and a compass. *Cell*. 2003;114(2):153-6.
- Mitchell, K.B. and Gallagher, J.J. (2012). Porcine bladder extracellular matrix for closure of large defect in a burn contracture release. *Journal Wound Care*. 9,454-6.
- Mondal S, Bakthavatsalam D, Steimle P, Gassen B, Rivero F, Noegel AA. Linking Ras to myosin function: RasGEF Q, a Dictyostelium exchange factor for RasB, affects myosin II functions. *J Cell Biol*. 2008;181(5):747-60.
- Ojalvo, L.S., Whittaker, C.A., Condeelis, J.S., and Pollard, J.W. (2009). Gene expression analysis of macrophages that facilitate tumor invasion supports a role for Wnt-signaling in mediating their activity in primary mammary tumors. *Immunology*. 184. 702-12.
- Park K.C., F. Rivero, R. Meili, S. Lee, F. Apone and Richard A Firtel (2004). —Rac regulation of chemotaxis and morphogenesis in Dictyostelium. *EMBO J*. 23: 4177-4189.
- Philips J, Herskowitz I. Identification of Kel1p, a kelch domain-containing protein involved in cell fusion and morphology in *Saccharomyces cerevisiae*. *J Cell Biol*. 1998;143(2):375-89.
- Prag, S, and J C. Adams. "Molecular phylogeny of the kelch-repeat superfamily reveals an expansion of BTB/kelch proteins in animals." *BMC Bioinformatics* 4.42 (2003). Web. 16 Nov. 2014.
- Radulescu, S., Ridgway, R.A., Cordero, J., Athineos, D., Salgueiro, P., Poulosom, R., Neuman, J., Jung, A., Patel, S., Woodgett, J., Barker, N., Pritchard, D.M., Oien, K., and Samson, O.J. (2012). Acute WNT signaling activation perturbs differentiation within the adult stomach and rapidly leads to tumour formation. *Oncogene*. 224.
- Sasaki, A., Chun, C., Takeda, K., and Firtel, R.A. (2004). Localized Ras signaling at the leading edge regulates PI3K, cell polarity, and directional cell movement. *Journal Cell Biology*. 167. 505-518.

- Sasaki AT, Firtel RA. Regulation of chemotaxis by the orchestrated activation of Ras, PI3K, and TOR. *Eur J Cell Biol.* 2006;85(9-10):873-9
- Schaap P. Evolutionary crossroads in developmental biology: *Dictyostelium discoideum*. *Development.* 2011;138(3):387-96.
- Segota I, Mong S, Neidich E, Rachakonda A, Lussenhop CJ, Franck C. High fidelity information processing in folic acid chemotaxis of *Dictyostelium amoebae*. *J R Soc Interface.* 2013;10(88):20130606.
- Shi C, Iglesias PA. Excitable behavior in amoeboid chemotaxis. *Wiley Interdiscip Rev Syst Biol Med.* 2013;5(5):631-42.
- Singh SP, Dhakshinamoorthy R, Jaiswal P, Schmidt S, Thewes S, Baskar R. The thyroxine inactivating gene, type III deiodinase, suppresses multiple signaling centers in *Dictyostelium discoideum*. *Dev Biol.* 2014;396(2):256-68.
- Sun T, Kim B, Kim LW. Glycogen Synthase Kinase 3 influences cell motility and chemotaxis by regulating PI3K membrane localization in *Dictyostelium*. *Dev Growth Differ.* 2013;55(8):723-34.
- Sutherland, C. (2011). What are the bona fide GSK3 substrates. *International Journal of Alzheimer's Disease.* 2011. 1-23.
- Teo, R., Lewis, K.J., Forde, J.E., Ryves, W.J., Reddy, J.V., Rogers, B.J., and Harwood, A.J. (2010). Glycogen synthase kinase-3 is required for efficient *Dictyostelium* chemotaxis. *Mol Bio Cell.* 21, 2788-2796.
- Towbin H., T. Staehelin and J. Gordon (1979). —Electrophoretic transfer of proteins from polyacrylamide gels to nitrocellulose sheets: procedure and some applications. *Proc Natl Acad Sci U S A.* 76(9): 4350–4354.
- Van Zijl, F., Krupitza, G., and Mikulits., W. (2011). Initial steps of metastasis: Cell invasion and endothelial transmigration. *Mutation Research* 728, 23-34.
- Vorotnikov, A.V. (2011). Chemotaxis: movement, direction, control. *Biochemistry (Mosc).* 76, 1528-1555.
- Wang, Y., Chen, C.L., and Iijima, M. (2011). Signaling mechanisms for Chemotaxis. *Dev Growth Differ.* 53, 495-502.
- Wessels D., E. Voss, N. Von Bergen, R. Burns, J. Stites and D. R. Soll (1998). —A Computer-Assisted System for Reconstructing and Interpreting the Dynamic Three-Dimensional Relationships of the Outer Surface, Nucleus and Pseudopods of Crawling Cells. *Cell Motil Cytoskeleton.* 41:225–246.
- Xiao Z, Zhang N, Murphy DB, Devreotes PN. Dynamic distribution of chemoattractant receptors in living cells during chemotaxis and persistent stimulation. *J Cell Biol.* 1997;139(2):365-74.

Zhang P, Wang Y, Sesaki H, Iijima M. Proteomic identification of phosphatidylinositol (3,4,5) triphosphate-binding proteins in *Dictyostelium discoideum*. *Proc Natl Acad Sci USA*. 2010;107(26):11829-34.